

# Higher-order tree-level amplitudes in the nonlinear sigma model

---

Johan Bijmens,<sup>a</sup> Karol Kampf,<sup>b</sup> Mattias Sjö<sup>a</sup>

<sup>a</sup>*Department of Astronomy and Theoretical Physics, Lund University,  
Sölvegatan 14A, Lund, Sweden*

<sup>b</sup>*Institute of Particle and Nuclear Physics, Charles University,  
V Holešovičkách 2, Prague, Czech Republic*

*E-mail:* [bijmens@thep.lu.se](mailto:bijmens@thep.lu.se), [karol.kampf@mff.cuni.cz](mailto:karol.kampf@mff.cuni.cz),  
[mattias.sjo@thep.lu.se](mailto:mattias.sjo@thep.lu.se)

ABSTRACT: We present a generalisation of the flavour-ordering method applied to the chiral nonlinear sigma model with any number of flavours. We use an extended Lagrangian with terms containing any number of derivatives, organised in a power-counting hierarchy. The method allows diagrammatic computations at tree-level with any number of legs at any order in the power-counting. Using an automated implementation of the method, we calculate amplitudes ranging from 12 legs at leading order,  $\mathcal{O}(p^2)$ , to 6 legs at next-to-next-to-leading order,  $\mathcal{O}(p^8)$ . In addition to this, we generalise several properties of amplitudes in the nonlinear sigma model to higher orders. These include the double soft limit and the uniqueness of stripped amplitudes.

---

## Contents

<b>1</b>	<b>Introduction</b>	<b>2</b>
<b>2</b>	<b>The nonlinear sigma model</b>	<b>3</b>
2.1	Restrictions due to fixed $N_f$ and dimensionality	5
<b>3</b>	<b>Flavour-ordering</b>	<b>6</b>
3.1	Some notation	7
3.2	Stripped vertex factors	8
3.3	Stripped amplitudes	9
3.4	Flavour-ordered diagrams	9
3.5	The singlet problem and its solution	12
3.6	Uniqueness of stripped amplitudes	14
<b>4</b>	<b>NLSM amplitudes</b>	<b>16</b>
4.1	Adler zeroes and soft limits	16
4.2	Generalised Mandelstam invariants	17
4.3	Diagram generation	19
<b>5</b>	<b>Explicit amplitudes</b>	<b>20</b>
5.1	4-point amplitudes	20
5.2	The $\mathcal{O}(p^2)$ 6- and 8-point amplitudes	22
5.3	The $\mathcal{O}(p^4)$ 6-point amplitude	23
5.4	Further amplitudes	23
<b>6</b>	<b>Conclusions</b>	<b>25</b>
<b>A</b>	<b>The NNLO NLSM Lagrangian</b>	<b>26</b>
A.1	Renormalisation	26
A.2	Explicit divergences	27
<b>B</b>	<b>The orthogonality of flavour structures</b>	<b>29</b>
<b>C</b>	<b>The double soft limit</b>	<b>31</b>
<b>D</b>	<b>Closed Mandelstam bases</b>	<b>32</b>
D.1	The basis for $R = \{2, 4\}$	32
D.2	The basis for $R = \{3, 3\}$	32
D.3	The basis for $R = \{2, 2, 2\}$	34

<b>E</b>	<b>Explicit amplitudes</b>	<b>34</b>
E.1	The $\mathcal{O}(p^6)$ 6-point amplitude	34
E.2	The $\mathcal{O}(p^2)$ 10-point amplitude	38
E.3	The $\mathcal{O}(p^2)$ 12-point amplitude	39

---

## 1 Introduction

In 1960, Gell-Mann and Lévy [1] proposed a number of models for mesons and nucleons. Two of these, the linear and nonlinear sigma models, were extended to highly general quantum field theories with many different applications. One of the most important application is interaction of mesons described by the nonlinear sigma model (NLSM) extended by Weinberg [2] and Gasser and Leutwyler [3, 4] into chiral perturbation theory ( $\chi$ PT). A recent introductory review is [5] and more introductory literature can be found at [6]. This effective field theory (EFT) of low-energy QCD is not only widely used today in many phenomenological applications, but also motivated further theoretical avenues for the beyond-standard-model physics such as technicolour and little Higgs models. Examples of recent work in  $\chi$ PT is the calculation of meson-meson scattering for a general number of flavours at two loops [7], and masses and decays up to next-to-next-to-leading order [8]. In this paper, we will push the study of this type of models in a different direction.

Even at tree-level, diagrammatic many-particle calculations in EFTs become very complicated due to the rapidly increasing number of terms in the effective Lagrangian, but can be facilitated with tools similar to those used for gluon scattering in perturbative QCD. In recent years, the renewal of interest in the  $S$ -matrix program for the gauge theory and gravity has in fact led to progress in both simplification of complicated technical calculations as well as discoveries of new properties [9]. The possibility to apply similar amplitude methods to EFTs started recently and is mainly connected with studies of the NLSM. First, it was demonstrated that it is indeed possible to employ recursive methods in [10], further studied and developed in [11]. The crucial ingredient in developing the recursive formula is the existence of the so-called Adler zero [12], the vanishing of scattering amplitudes for soft momenta of Goldstone bosons (pions for NLSM), as a consequence of a spontaneous symmetry breaking in EFT. The argument can be also inverted and used for classification of the allowed space of EFT theories based on their soft properties. It turned out that the leading order of NLSM is one important representative of exceptional EFTs. The exceptional status of those theories is connected with the fact that all their interaction vertices are uniquely fixed by a single coupling constant, most conveniently the lowest four-point vertex. This can be labelled as a soft-bootstrap program, studied and developed in recent years by several groups [13–15]. It represents a rebirth of similar attempts at the end of the 1960s [16–18].

The exceptional theories have also appeared in completely different context, the so-called CHY scattering equation [19], studied more recently also in [20]. This indeed suggests their uniqueness, and though of completely different nature, it hints to deeper connections

with gauge theory and gravity. It is probably one of the main motivations behind the recent increase of activities in studying theoretical properties of NLSM: [21–33]. This effort demonstrates the importance of NLSM; however, these studies mainly concentrated only on the leading, two-derivative ( $\mathcal{O}(p^2)$ ) order. As pointed out in [15], it is important to expand the on-shell soft bootstrap program to higher orders. Our work aims in this direction. An early attempt is [34] and one that appeared during the writing up of this paper is [35].

We will mainly focus on the problem of calculating scattering amplitudes at tree-level with increasing number of legs and orders, with possible flavour splitting, i.e. beyond single-trace amplitudes. Using recursion relations, tree-level amplitudes based on the leading-order term in the Lagrangian have been computed with up to 10 external particles [36]. Using more general recursion relations based on soft limits [11], 6-particle tree-level interactions have been computed using the next-to-leading-order Lagrangian [15]. These methods suffer limitations when higher-order Lagrangian terms are used, and can not handle loops.

In this paper, we generalise an enhanced diagrammatic method called flavour-ordering, which was introduced in [36]. We apply it to a generalised version of the  $SU(N)$  or  $U(N)$  chiral NLSM, which includes terms with arbitrarily high power-counting order in the effective Lagrangian. This generalisation corresponds to removing all external fields from the general  $\chi$ PT Lagrangian. The method allows computation of tree-level amplitudes with any number of external particles using Lagrangian terms of any order, and is valid also beyond tree-level. It is significantly more efficient than a brute-force Feynman diagram approach, and the caveats that appear beyond the leading order can be handled with simple rules. Preliminary results can be found in the Lund university master thesis [37].

In section 2, we describe the NLSM and introduce our notation. Our main new results on the method side are described in section 3 and 4. Section 3 discusses our generalization of flavour-ordering, while section 4 discusses how this can be used to calculate more complex amplitudes as well as the kinematic methods needed. Section 5 discusses the amplitudes we have calculated using our methods; the longer expressions are relegated to appendix E and the supplementary material [38]. Our main conclusions are reviewed in section 6. The Lagrangians are given in appendix A, together with some results regarding renormalisation of the amplitudes. Appendix B contains the proof of the orthogonality of flavour structures. The double soft limit with multiple traces is derived in appendix C, and appendix D derives the minimal bases of kinematic variables used in the amplitude calculations.

## 2 The nonlinear sigma model

The nonlinear sigma model describes the Nambu-Goldstone bosons that arise when a global symmetry group  $G$  is broken to a subgroup  $H$ . Each configuration of the Nambu-Goldstone fields can be uniquely mapped to an element of the coset space  $G/H$ , and from each such coset, a representative  $\xi(\phi)$  may be chosen to represent the field configuration  $\phi$ .

In the context of low-energy QCD, the group  $G$  is the chiral group  $SU(N_f)_L \times SU(N_f)_R$ , which is a global symmetry of the massless QCD Lagrangian with  $N_f$  quark

flavours. It is broken to the diagonal subgroup  $H = SU(N_f)_V$ , so the coset space  $G/H$  is isomorphic to  $SU(N_f)$ . With a chiral decomposition of the coset representatives,  $\xi = (\xi_L, \xi_R)$ , we may represent the Nambu-Goldstone fields with the unitary matrix  $u(\phi) = \xi_R(\phi) = \xi_L^\dagger(\phi)$  parametrised as

$$u(\phi) = \exp\left(\frac{i\Phi(\phi)}{F\sqrt{2}}\right), \quad \Phi(\phi) = t^a \phi^a \quad (2.1)$$

with the flavour index with  $a$  running from 1 to  $N_f^2 - 1$ . Here,  $t^a$  are the generators of  $SU(N_f)$ , and  $F$  is a constant.<sup>1</sup> We use Einstein's summation notation without distinction between upper and lower flavour indices, and use the following normalisation for the generators:

$$\langle t^a t^b \rangle = \delta^{ab}, \quad [t^a, t^b] = i f^{abc} t^c, \quad (2.2)$$

where  $\langle \dots \rangle$  denotes a trace over internal indices. Here,  $f^{abc}$  are the totally antisymmetric structure constants of  $SU(N_f)$ . With this convention, the  $SU(2)$  generators can be chosen such that they relate to the Pauli matrices as  $t^a = \sigma^a / \sqrt{2}$ ,  $f^{abc} = \epsilon^{abc} \sqrt{2}$ . Likewise, the  $SU(3)$  generators can be chosen in terms of the Gell-Mann matrices like  $t^a = \lambda^a / \sqrt{2}$ .

Under a chiral transformation  $g = (g_L, g_R)$ ,  $u(\phi)$  transforms as

$$u \xrightarrow{g} g_R u h^\dagger(u, g) = h(u, g) u g_L, \quad (2.3)$$

where the compensating transformation  $h(u, g) \in H$  is defined by the above relation.

When constructing the most general symmetry-consistent Lagrangian, it is more convenient to replace  $u$  by

$$u_\mu = i \left( u^\dagger \partial_\mu u - u \partial_\mu u^\dagger \right), \quad u_\mu \xrightarrow{g} h(u, g) u_\mu h(u, g)^\dagger, \quad (2.4)$$

which was introduced in this context by [39]. Higher derivatives are applied through the covariant derivative

$$\nabla_\mu X = \partial_\mu X + [\Gamma_\mu, X], \quad \Gamma_\mu = \frac{1}{2} \left( u^\dagger \partial_\mu u + u \partial_\mu u^\dagger \right), \quad (2.5)$$

which has the convenient properties

$$X \xrightarrow{g} h X h^\dagger \Rightarrow \nabla_\mu X \xrightarrow{g} h \nabla_\mu X h^\dagger, \quad \nabla_\mu u_\nu - \nabla_\nu u_\mu = 0. \quad (2.6)$$

Note that we do not include the external fields that are used in chiral perturbation theory.

The Lagrangian is often written using derivatives of  $U(\phi) = u(\phi)^2$  and its conjugate. It is possible to convert directly between  $\partial_\mu U^{(\dagger)}$  and  $u_\mu$  by using unitarity:

$$\partial_\mu U^\dagger \partial_\nu U = - (U^\dagger \partial_\mu U) (U^\dagger \partial_\nu U), \quad U^\dagger \partial_\mu U = u^\dagger u^\dagger \partial_\mu u u - \partial_\mu u^\dagger u = -i u^\dagger u_\mu u. \quad (2.7)$$

This makes  $\partial_\mu U^\dagger \partial_\nu U$  wholly interchangeable with  $u_\mu u_\nu$  inside a trace.

---

<sup>1</sup>The above expression for  $u(\phi)$  is only one of many possible parametrisations, but is the most common.

With the above definitions, the simplest valid term in the NLSM Lagrangian is

$$\mathcal{L}_2 = \frac{F^2}{4} \langle u_\mu u^\mu \rangle, \quad (2.8)$$

where the constant in front is fixed by the canonical normalisation of the kinetic term.

Beyond this, there is an infinite sequence of increasingly complex terms permitted by the chiral symmetries<sup>2</sup>. We also impose parity ( $P$ ), charge-conjugation ( $C$ ) and Lorentz invariance. We restrict to the sector that involves an even number of Levi-Civita tensors ( $\epsilon_{\mu\nu\alpha\beta}$ ), which can always be rewritten in terms of the Minkowski metric only. The terms can be organised into a hierarchy based on power counting in the momentum scale  $p$ . Since each derivative in the Lagrangian brings down one factor of  $p$  into an amplitude, both  $u_\mu$  and  $\nabla_\mu$  are  $\mathcal{O}(p)$  and the power-counting at the Lagrangian level is simply counting derivatives. Thus, we may split the Lagrangian as

$$\mathcal{L} = \sum_{n=1}^{\infty} \mathcal{L}_{2n}, \quad (2.9)$$

where  $\mathcal{L}_{2n}$  is  $\mathcal{O}(p^{2n})$  and contains  $2n$  derivatives carrying  $n$  pairs of Lorentz indices. Assuming a low momentum scale, we may then ignore all terms above a certain  $n$ .

The four-derivative  $\mathcal{O}(p^4)$  Lagrangian is, for general  $N_f$  [3, 4, 40],

$$\mathcal{L}_4 = L_0 \langle u_\mu u_\nu u^\mu u^\nu \rangle + L_1 \langle u_\mu u^\mu \rangle \langle u_\nu u^\nu \rangle + L_2 \langle u_\mu u_\nu \rangle \langle u^\mu u^\nu \rangle + L_3 \langle u_\mu u^\mu u_\nu u^\nu \rangle. \quad (2.10)$$

The  $L_i$  are independent coupling constants, so-called low-energy constants (LECs). It is in principle possible to derive the LECs from any underlying theory (e.g. QCD), but in practice, they are unknown parameters that must be measured by experiments or lattice simulations.

The Lagrangian is known also at  $\mathcal{O}(p^6)$  and  $\mathcal{O}(p^8)$ . The latter is the first 135 terms in the  $\chi$ PT Lagrangian of [41]; the former has only been published with different notation and formulated in a way that gives redundant terms when naïvely reduced to the NLSM [40]. A more compatible version, constructed in conjunction with [41], is given in appendix A. The Lagrangian at  $\mathcal{O}(p^{10})$  and above has not been studied.

## 2.1 Restrictions due to fixed $N_f$ and dimensionality

The Lagrangians discussed above are the most general ones. They are valid in any dimension and for a generic number of flavours.

When  $N_f$  is small, the Cayley-Hamilton theorem gives additional linear relations that reduce the number of independent terms. The theorem states that for any  $N_f \times N_f$  matrix  $M$ , the characteristic polynomial

$$p(\lambda) = \det(\lambda \mathbb{1} - M), \quad (2.11)$$

---

<sup>2</sup>Many authors refer to  $\mathcal{L}_2$  as the full Lagrangian of the NLSM. We instead use “the NLSM” to refer to the more general version, which includes also terms with more derivatives.

which is zero whenever  $\lambda$  is an eigenvalue of  $M$ , is also satisfied by  $M$ , i.e.  $p(M) = 0$  when viewed as a matrix polynomial. When  $N_f = 2$ , this implies the identity

$$\{A, B\} = \langle AB \rangle, \quad (2.12)$$

for traceless  $2 \times 2$  matrices  $A, B$ . When  $N_f = 3$ , the identity is

$$\sum_{\text{permutations of } \{ABC\}} \langle ABCD \rangle = \sum_{\text{cyclic permutations of } \{ABC\}} \langle AB \rangle \langle CD \rangle, \quad (2.13)$$

for traceless matrices. The relations when  $\langle A \rangle \neq 0$  used in [40, 41] contain many more terms.

As an example, we may choose  $A = C = u_\mu$  and  $B = D = u_\nu$ ; these are traceless as a consequence of the identity  $\partial_\mu \det(A) = \det(A) \langle A^{-1} \partial_\mu A \rangle$ , which holds for any invertible  $A$ , and which reduces to  $\langle A^\dagger \partial_\mu A \rangle = 0$  when  $A \in SU(N_f)$ .

The  $N_f = 2$  identity allows for the elimination of all Lagrangian terms containing a product of two or more traces from any  $\mathcal{L}_{2n}$ ; for instance,  $L_1$  and  $L_2$  may be eliminated from  $\mathcal{L}_4$ . The  $N_f = 3$  identity allows for the removal of a single term from  $\mathcal{L}_4$ , 7 terms from  $\mathcal{L}_6$ , and so on. The standard choice is to remove the  $L_0$ -term of (2.10) for  $N_f = 3$  [4], and the  $L_0$ - and  $L_3$ -terms for  $N_f = 2$  [3].

When the spacetime dimension  $D$  is finite, the Schouten identity implies

$$(f^{\mu_1 \mu_2 \dots \mu_k} u_{\mu_1} u_{\mu_2} \dots u_{\mu_k})^2 = 0 \quad \text{if } k > D, \quad (2.14)$$

where  $f^{\mu_1 \mu_2 \dots \mu_k}$  is antisymmetric in all its indices. This results in additional linear relations among the terms in  $\mathcal{L}_{2k}$  for  $k > D$ . For  $D = 4$ , this does not affect any of the currently known orders. In the sector involving a single Levi-Civita tensor it already removes a large number of terms at  $\mathcal{O}(p^6)$ .

### 3 Flavour-ordering

With the structure of the NLSM established, we are ready to use it for perturbative calculations of scattering amplitudes. However, the infinite number of interaction terms requires the use of some scheme for restricting it to a manageable subset. Even then, the resulting vertex factors are very intricate, both in their dependence on the particle momenta, and in their group-algebraic structure. This leaves only the simplest Feynman diagrams tractable by hand, and even computer algebra becomes highly time-consuming when tackling more complicated cases directly.

In this section, we will direct much effort towards the development of simpler ways to perform these calculations. As we will see, the group-algebraic structure of the flavour indices carried by the particles can be used to condense an amplitude into a much more easily manageable expression, for which simpler calculation rules exist. We will mostly follow the derivation of  $\mathcal{O}(p^2)$  flavour-ordering as presented in [36], but insert the notation to support our own generalisations to higher-order vertices.

### 3.1 Some notation

In this section, we will need a compact notation for writing the flavour structures of scattering amplitudes. A flavour structure is a product of one or more traces containing group generators carrying the flavour indices of the external particles in some order. We will represent this as

$$\mathcal{F}_\sigma(r_1, r_2, \dots) = \langle t^{a_{\sigma(1)}} \dots t^{a_{\sigma(r_1)}} \rangle \langle t^{a_{\sigma(r_1+1)}} \dots t^{a_{\sigma(r_1+r_2)}} \rangle \dots \quad (3.1)$$

The  $i$ th trace contains  $r_i$  generators, ordered by a permutation  $\sigma \in \mathcal{S}_n$ . For example,  $\langle a_1 a_3 \rangle \langle a_2 a_4 \rangle = \mathcal{F}_{1324}(2, 2)$ , and  $\langle a_1 a_2 \dots a_n \rangle = \mathcal{F}_{\text{id}}(n)$ , where  $\text{id}(i) = i$  is the identity permutation.

We encapsulate the  $r_i$  in  $R = \{r_1, r_2, \dots, r_{|R|}\}$ . We call  $R$  a *flavour splitting*.  $|R|$  is the number of traces in the flavour structure, and we write  $\mathcal{F}_\sigma(R)$  rather than  $\mathcal{F}_\sigma(r_1, \dots)$ . For a structure with  $n$  indices, we impose the restrictions

$$\sum_{i=1}^{|R|} r_i = n, \quad r_1 \leq r_2 \leq \dots \leq r_{|R|}. \quad (3.2)$$

The latter limits the number of equivalent ways to write a flavour structure.

Since traces are cyclic,  $\mathcal{F}_\sigma(R)$  will be invariant under cyclic permutations of the indices inside each trace. If  $r_i = r_j$ , it will also be invariant under swapping the contents of the  $i$ th and  $j$ th trace. As a generalisation of the cyclic group  $\mathbb{Z}_n$ , we define  $\mathbb{Z}_R$  to be the group of all permutations under which  $\mathcal{F}_\sigma(R)$  is invariant. For instance,

$$\begin{aligned} \mathbb{Z}_{\{2,2\}} &= \{12\ 34, 21\ 34, 12\ 43, 21\ 43, 34\ 12, 43\ 12, 34\ 21, 43\ 21\}, \\ \mathbb{Z}_{\{2,4\}} &= \{12\ 3456, 21\ 3456, 12\ 4563, 21\ 4563, 12\ 5634, 21\ 5634, 12\ 6345, 21\ 6345\}, \end{aligned} \quad (3.3)$$

where we label a permutation by how  $12 \dots n$  ends up. We have inserted spaces between blocks of indices corresponding to different traces to make it more legible.

In this notation, we generalise the notion of two permutations being equivalent modulo a cyclic permutation: we write  $\sigma \equiv \rho \pmod{\mathbb{Z}_R}$  if  $\mathcal{F}_\sigma(R) = \mathcal{F}_\rho(R)$ . For instance,  $1234 \equiv 2341 \pmod{\mathbb{Z}_{\{4\}}}$  and  $1234 \equiv 2134 \pmod{\mathbb{Z}_{\{2,2\}}}$ .

$\mathbb{Z}_{\{2,2\}}$  is isomorphic to the dihedral group  $D_4$ . Other  $\mathbb{Z}_R$  are not isomorphic to such well-known groups, but  $\mathbb{Z}_{\{2,4\}} \simeq \mathbb{Z}_2 \times \mathbb{Z}_4$ , and in general,  $\mathbb{Z}_R \simeq \mathbb{Z}_{r_1} \times \mathbb{Z}_{r_2} \times \dots$  whenever all  $r_i$  are different. When some  $r_i$  are equal (say,  $m$  in a row), the group will be non-abelian and isomorphic to a semidirect product, e.g.  $\mathbb{Z}_{\{2,2,2\}} \simeq (\mathbb{Z}_2 \times \mathbb{Z}_2 \times \mathbb{Z}_2) \rtimes \mathcal{S}_3$ . In general,  $\mathbb{Z}_R \simeq (\mathbb{Z}_{r_1} \times \mathbb{Z}_{r_2} \times \dots) \rtimes (\mathcal{S}_{m_1} \times \mathcal{S}_{m_2} \times \dots)$ , where each  $m_j$  is the length of a stretch of equal  $r_i$ .<sup>3</sup>

---

<sup>3</sup>The proof follows from the following definition of the semidirect product: if a group  $G$  has a subgroup  $H$  and a normal subgroup  $N$ , then  $G = N \rtimes H$  if  $G = \{nh \mid n \in N, h \in H\}$  and  $N \cap H = e$ , the identity element. The groups  $N \simeq (\mathbb{Z}_{r_1} \times \dots)$  of cyclings within traces and  $H \simeq (\mathcal{S}_{m_1} \times \dots)$  of swaps of equal-size traces are clearly subgroups of  $G = \mathbb{Z}_R$ , and  $N$  is normal since  $gnh^{-1} \in N$  for any  $n \in N, g \in G$  — any trace swaps in  $g$  are cancelled by  $g^{-1}$ , leaving only cyclings. Any permutation in  $\mathbb{Z}_R$  is the composition of a cycling and a trace swap, and the only element shared by  $N$  and  $H$  is  $\text{id}$ , which completes the proof.

### 3.2 Stripped vertex factors

Each term in the Lagrangian will produce an infinite tower of interaction vertices with increasingly many legs. Due to parity and the absence of Levi-Civita tensors, only terms with an even number of legs are produced. If the Lagrangian term contains a product of several traces, the flavour indices of the corresponding vertices will be distributed between the same number of traces in multiple ways. If a trace contains an even number of  $u_\mu$ 's in the Lagrangian, the corresponding trace in the vertices will only contain an even number of indices, again from parity.

We will organise the vertices by their power-counting order and flavour splitting. For instance, in the expansion of  $\mathcal{L}_2$  (2.8),

$$\mathcal{L}_2 = \frac{1}{2} \langle t^a t^b \rangle \partial_\mu \phi^a \partial^\mu \phi^b + \frac{1}{F^2} \langle t^a t^b t^c t^d \rangle \left( \frac{1}{6} \phi^a \partial_\mu \phi^b \phi^c \partial^\mu \phi^d - \frac{1}{12} \phi^a \phi^b \partial_\mu \phi^c \partial^\mu \phi^d \right) + \dots, \quad (3.4)$$

both terms attached to the 4-index trace will be part of the  $\mathcal{O}(p^2)$  vertex with splitting  $R = \{4\}$ , which we label  $\mathcal{V}_{2,\{4\}}^{abcd}$ , a vertex (factor). At order  $p^m$ , a specific flavour splitting  $R$  for a vertex with  $n$  legs, and thus  $n$  flavour indices  $a_i$ , will have a vertex factor  $\mathcal{V}_{m,R}^{a_1 \dots a_n}$ . It will in general contain contributions from many different Lagrangian terms, but we treat it as a single factor for the purposes of Feynman diagrams.

We can further organise the contents of an  $n$ -point  $\mathcal{O}(p^m)$  vertex by flavour structure, i.e. all possible distributions of the  $n$ -flavour indices over the flavour splitting  $R$ :

$$\mathcal{V}_{m,R}^{a_1 a_2 \dots a_n}(p_1, p_2, \dots, p_n) = \sum_{\sigma \in \mathcal{S}_n / \mathbb{Z}_R} \mathcal{F}_\sigma(R) \mathcal{V}_{m,R,\sigma}(p_1, p_2, \dots, p_n), \quad (3.5)$$

where  $\mathcal{V}_{m,R,\sigma}$  contains whatever kinematic factors come attached to  $\mathcal{F}_\sigma(R)$ . Due to the derivatives, the kinematic factors  $\mathcal{V}_{m,R,\sigma}$  are functions of the momenta  $p_i$  of the interacting particles. Here and in all other places, we treat all momenta as ingoing. Since  $\mathcal{F}_\sigma(R)$  is invariant under  $\mathbb{Z}_R$ , the kinematic factors must also have this symmetry, i.e.

$$\mathcal{V}_{m,R,\sigma}(p_1, p_2, \dots, p_n) = \mathcal{V}_{m,R,\sigma}(p_{\rho(1)}, p_{\rho(2)}, \dots, p_{\rho(n)}) \quad (3.6)$$

for any  $\rho \in \mathbb{Z}_R$ . Also, Bose symmetry implies that the act of rearranging the legs of the vertex by any permutation  $\rho \in \mathcal{S}_n$  must have the effect

$$\mathcal{V}_{m,R,\sigma \circ \rho}(p_1, p_2, \dots, p_n) = \mathcal{V}_{m,R,\sigma}(p_{\rho(1)}, p_{\rho(2)}, \dots, p_{\rho(n)}), \quad (3.7)$$

where  $\circ$  denotes composition of permutations. Specifically,

$$\mathcal{V}_{m,R,\sigma}(p_1, p_2, \dots, p_n) = \mathcal{V}_{m,R}(p_{\sigma(1)}, p_{\sigma(2)}, \dots, p_{\sigma(n)}), \quad (3.8)$$

where  $\mathcal{V}_{m,R} = \mathcal{V}_{m,R,\text{id}}$  is called a *stripped* vertex factor.<sup>4</sup> It contains all the necessary

<sup>4</sup>The word “stripped” is typical in the context of EFTs. For the analogous concept in perturbative QCD (where “flavour” is replaced by “colour”), the word “primitive” is used instead; see e.g. [42, 43]. In older literature, the word “dual” is common.

information of the full vertex factor, but is only a kinematic factor with no flavour structure. It can be “dressed” into a full vertex factor by the simple act of multiplying by  $\mathcal{F}_{\text{id}}(R)$  and then summing over all  $\sigma \in \mathcal{S}_n/\mathbb{Z}_R$ .

A stripped vertex factor has the property of being *flavour-ordered*, since it is the kinematic factor attached to  $\mathcal{F}_{\text{id}}(R)$ , where all flavour indices are sorted in ascending order. Thanks to this, its explicit form can be derived by expanding the relevant Lagrangian terms and discarding all terms where any flavour index appears out of order. This saves a significant amount of work for the more complicated vertices.

Stripped vertices serve as the first ingredient in our method. In the following sections, we treat diagrams and amplitudes along the same lines.

### 3.3 Stripped amplitudes

Like the vertices, we may organise the diagrams by their power-counting order and flavour structure. The order can be determined by using Weinberg’s power-counting formula,

$$D = 2 + 2L + \sum_d (d - 2)N_d, \quad (3.9)$$

which states that a diagram containing  $L$  loops and  $N_d$   $\mathcal{O}(p^d)$  vertices is  $\mathcal{O}(p^D)$  overall. Due to the form  $(d - 2)$ , a diagram may contain any number of  $\mathcal{O}(p^2)$  vertices without changing its order.

As for the vertex factors, we may decompose the  $\mathcal{O}(p^m)$   $n$ -point amplitude as

$$\mathcal{M}_{m,n}^{a_1 a_2 \dots a_n}(p_1, p_2, \dots, p_n) = \sum_{R \in \mathcal{R}(m,n)} \sum_{\sigma \in \mathcal{S}_n/\mathbb{Z}_R} \mathcal{F}_\sigma(R) \mathcal{M}_{m,R,\sigma}(p_1, p_2, \dots, p_n), \quad (3.10)$$

where  $\mathcal{M}_{m,R,\sigma}$  carries all kinematic factors, and  $\mathcal{R}(m,n)$  contains all flavour splittings that contribute to the amplitude. Its contents will become apparent when drawing diagrams.

The direct analogues of (3.6–3.8) hold also for  $\mathcal{M}_{m,R,\sigma}$ , and we may similarly define the *stripped amplitude*  $\mathcal{M}_{m,R}$  with the property

$$\mathcal{M}_{N,R,\sigma}(p_1, p_2, \dots, p_n) = \mathcal{M}_{m,R}(p_{\sigma(1)}, p_{\sigma(2)}, \dots, p_{\sigma(n)}). \quad (3.11)$$

It is sufficient to compute the stripped amplitude, since summing over flavour splittings and permutations,

$$\mathcal{M}_{m,n}^{a_1 a_2 \dots a_n}(p_1, p_2, \dots, p_n) = \sum_{R \in \mathcal{R}(N,n)} \sum_{\sigma \in \mathcal{S}_n/\mathbb{Z}_R} \mathcal{F}_\sigma(R) \mathcal{M}_{m,R}(p_{\sigma(1)}, p_{\sigma(2)}, \dots, p_{\sigma(n)}), \quad (3.12)$$

gives the full amplitude.

### 3.4 Flavour-ordered diagrams

Due to its relative simplicity, the stripped amplitude serves as the target of our methods. Like the stripped vertex factors, it is flavour-ordered, so when calculating it, we may discard all terms where two flavour indices appear out of order. We can derive further

simplifications by studying how the flavour structures behave when two sub-diagrams are joined by propagators. The NLSM Feynman rule for a propagator with momentum  $q$  is

$$\begin{array}{c} q \\ \hline a \quad b \end{array} = \frac{i\delta^{ab}}{q^2 + i\epsilon}, \quad (3.13)$$

so the flavour structures are simply contracted by the delta. For  $SU(N_f)$ , the contraction can be performed through the Fierz identity,

$$t_{ij}^a t_{kl}^a = \delta_{il}\delta_{jk} - \frac{1}{N_f}\delta_{ij}\delta_{kl}, \quad (3.14)$$

where  $ijkl$  are the internal indices of the generators. Inside traces, the identity implies

$$\langle Xt^a \rangle \langle t^a Y \rangle = \langle XY \rangle - \frac{1}{N_f} \langle X \rangle \langle Y \rangle, \quad (3.15)$$

$$\langle Xt^a Y t^a \rangle = \langle X \rangle \langle Y \rangle - \frac{1}{N_f} \langle XY \rangle \quad (3.16)$$

for arbitrary  $X$  and  $Y$ . For future reference, we will name the first term on the right-hand side the *multiplet term* and the second term (containing  $N_f^{-1}$ ) the *singlet term*. In  $U(N_f)$ , the corresponding identities contain only the multiplet term.

For tree-level diagrams, (3.15) is the relevant identity. Its multiplet term preserves the ordering of  $X$  and  $Y$ ; the singlet term does not, but we will ignore it for now and deal with it in section 3.5. We then see that the stripped amplitude only gets contributions from stripped vertex factors (if  $X$  or  $Y$  is not flavour-ordered, neither is  $XY$ ) that are combined in ways that maintain their flavour-ordering. In a diagrammatic view, this is rather intuitive to achieve; for instance, the following constitutes all the distinct ways to assemble two 4-point vertices into an  $\mathcal{O}(p^2)$  6-point diagram:

$$\begin{array}{ccc} \begin{array}{c} 1 \\ 2 \\ 3 \end{array} \begin{array}{c} \diagup \\ \diagdown \end{array} \begin{array}{c} \diagdown \\ \diagup \end{array} \begin{array}{c} 6 \\ 5 \\ 4 \end{array} & \begin{array}{c} 2 \\ 3 \\ 4 \end{array} \begin{array}{c} \diagup \\ \diagdown \end{array} \begin{array}{c} \diagdown \\ \diagup \end{array} \begin{array}{c} 1 \\ 6 \\ 5 \end{array} & \begin{array}{c} 3 \\ 4 \\ 5 \end{array} \begin{array}{c} \diagup \\ \diagdown \end{array} \begin{array}{c} \diagdown \\ \diagup \end{array} \begin{array}{c} 2 \\ 1 \\ 6 \end{array} \end{array} \quad (3.17)$$

The labels on the legs refer to external momenta and flavour indices. Flavour-ordering corresponds to having all indices in cyclic order around the diagram labelled counterclockwise; we will keep this convention in the remainder. These three labellings give distinct kinematic factors, e.g. they have distinct propagator momenta  $(p_1 + p_2 + p_3)^2$ ,  $(p_2 + p_3 + p_4)^2$ , and  $(p_3 + p_4 + p_5)^2$ , respectively. Due to the symmetry of the diagram, the remaining three cyclic permutations of the labels are not distinct from these three. All other labellings are not flavour-ordered, and can be ignored.

For compactness, we will draw flavour-ordered diagrams with unlabelled legs. These are defined as the sum over all distinct flavour-ordered ways to label them. Equivalently, they can be defined as any flavour-ordered labelling, summed over  $\mathbb{Z}_R$ , and divided by the factor needed to account for symmetry. For 4, 6 and 8 particles at  $\mathcal{O}(p^2)$ , the flavour-

ordered diagrams are

$$(3.18)$$

respectively. The second 6-point diagram is the sum of the three in (3.17). Stripped vertex factors are completely symmetric under their respective  $\mathbb{Z}_R$  by virtue of (3.6), so single-vertex diagrams always have only one distinct labelling. Therefore, the 4-point diagram and the first 6-point diagram in (3.18) should not be summed over other labellings. The 8-point diagrams have 1, 8, 4, and 8 distinct labellings, respectively, as can be seen from their symmetry. Note that since the order of the legs of a stripped vertex factor matters, the last two diagrams are distinct.

Above  $\mathcal{O}(p^2)$ , we begin to encounter flavour-split vertices, but they can be integrated into the flavour-ordering routine. We still label the legs according to the identity permutation, but instead of summing over cyclic permutations, we sum over  $\mathbb{Z}_R$ , and once again only consider distinct labellings.

At higher orders, we also need to distinguish vertices of different order, which is done by attaching a number to all vertices above  $\mathcal{O}(p^2)$ . In order to distinguish vertices with split flavour structures, we leave a gap in the vertex, so that each contiguous piece of a diagram resides in a single trace. For instance, the 4-point  $\mathcal{O}(p^4)$  diagrams are

$$(3.19)$$

for  $R = \{4\}$  and  $R = \{2, 2\}$ , respectively. Neither diagram has more than one distinct labelling, since they contain only a single vertex each. The four lines in the right diagram are still kinematically connected, but are separated flavour-wise. Since there is a direct correspondence between traces in a flavour structure and contiguous pieces of a diagram, we will simply refer to the pieces as *traces*.

Some adjustment is needed when handling split diagrams. Since  $\langle X \rangle \langle Y \rangle = \langle Y \rangle \langle X \rangle$ , the traces may “float” to different positions around the same vertex. For instance,

$$(3.20)$$

are the same. By our conventions, the distinct labellings of this diagram are

$$(3.21)$$

Labels 1 and 2 are applied to the smaller trace (as per (3.2)), and no cycling is needed due to the symmetry of the vertex. Labels 3456 must be summed over all four cyclings,

since each cyclings gives a different propagator. No other labelling is flavour-ordered; in particular,

$$\begin{array}{c}
 5 \\
 \diagdown \\
 \text{---} 4 \\
 \diagup \\
 6 \\
 \text{---} \\
 \diagdown \\
 1
 \end{array}
 \text{---}
 \begin{array}{c}
 \diagup \\
 4 \\
 \diagdown \\
 3 \\
 \text{---} \\
 \diagup \\
 2
 \end{array}
 , \tag{3.22}$$

which would be valid on a single-trace diagram, should not be counted, since it has flavour structure  $\mathcal{F}_{\text{id}}(4, 2)$  in disagreement with (3.2). Including it would be double-counting when summing over all  $\sigma$  in (3.12), since it is obtained from (3.21) via a permutation in  $\mathcal{S}_6/\mathbb{Z}_{\{2,4\}}$ .

Extra caveats sometimes show up. For instance, the two  $\mathcal{O}(p^4)$  diagrams

$$\begin{array}{c}
 \diagup \\
 \diagdown \\
 \text{---} 4 \\
 \diagup \\
 \diagdown
 \end{array}
 \text{---}
 \begin{array}{c}
 \diagup \\
 \diagdown \\
 \text{---} 4 \\
 \diagup \\
 \diagdown
 \end{array}
 \quad
 \begin{array}{c}
 \diagup \\
 \diagdown \\
 \text{---} 4 \\
 \diagup \\
 \diagdown
 \end{array}
 \tag{3.23}$$

emerge from different orientations of the same three vertices, but have completely different flavour structure and properties. In the first diagram, the smaller trace should not be cycled at all, and the larger trace only halfway, since it is symmetric (compare to the  $\mathcal{O}(p^2)$  6-point diagram). In the second diagram, all  $4 \cdot 4$  combined cyclings of the two traces are distinct, but due to the symmetry of the diagram, swapping them, e.g.

$$\begin{array}{c}
 8 \\
 \diagdown \\
 \text{---} 4 \\
 \diagup \\
 2 \\
 \text{---} \\
 \diagdown \\
 3
 \end{array}
 \text{---}
 \begin{array}{c}
 \diagup \\
 \diagdown \\
 \text{---} 4 \\
 \diagup \\
 \diagdown \\
 5
 \end{array}
 \quad
 \longleftrightarrow
 \quad
 \begin{array}{c}
 5 \\
 \diagdown \\
 \text{---} 4 \\
 \diagup \\
 6 \\
 \text{---} \\
 \diagdown \\
 7
 \end{array}
 \text{---}
 \begin{array}{c}
 \diagup \\
 \diagdown \\
 \text{---} 4 \\
 \diagup \\
 \diagdown \\
 1
 \end{array}
 \tag{3.24}$$

does not produce a distinct kinematic structure and should not be counted.

In the  $\mathcal{O}(p^6)$  diagrams

$$\begin{array}{c}
 \diagup \\
 \diagdown \\
 \text{---} 4 \\
 \diagup \\
 \diagdown
 \end{array}
 \text{---}
 \begin{array}{c}
 \diagup \\
 \diagdown \\
 \text{---} 4 \\
 \diagup \\
 \diagdown
 \end{array}
 \quad
 \begin{array}{c}
 \diagup \\
 \diagdown \\
 \text{---} 6 \\
 \diagup \\
 \diagdown
 \end{array}
 , \tag{3.25}$$

the component of  $\mathbb{Z}_R$  that swaps equal-size traces does play a role. In the first diagram, we may place either 12 or 34 in the trace straddling the propagator, and we must sum over both placements. In addition to that, we must sum over cyclings of the trace that straddles the propagator. In the second diagram, the two smaller traces are equivalent under the  $\mathbb{Z}_{\{2,2,2\}}$  symmetry of the vertex, and we should not sum over both ways of placing the labels 12 and 34.

### 3.5 The singlet problem and its solution

The construction of flavour-ordered diagrams hinges heavily on the use of (3.15), or specifically the multiplet term,  $\langle XY \rangle$ . The singlet term,  $\langle X \rangle \langle Y \rangle / N_f$ , threatens the notion that the stripped amplitude is given by exactly the flavour-ordered diagrams. Consider the diagrams

$$\begin{array}{c}
 1 \\
 \diagdown \\
 \text{---} \\
 \diagup \\
 2 \\
 \text{---} \\
 \diagdown \\
 3
 \end{array}
 \text{---}
 \begin{array}{c}
 \diagup \\
 \diagdown \\
 \text{---} 6 \\
 \diagup \\
 \diagdown \\
 4
 \end{array}
 \quad
 \begin{array}{c}
 2 \\
 \diagdown \\
 \text{---} \\
 \diagup \\
 3 \\
 \text{---} \\
 \diagdown \\
 4
 \end{array}
 \text{---}
 \begin{array}{c}
 \diagup \\
 \diagdown \\
 \text{---} 1 \\
 \diagup \\
 \diagdown \\
 5
 \end{array}
 \quad
 \begin{array}{c}
 3 \\
 \diagdown \\
 \text{---} \\
 \diagup \\
 1 \\
 \text{---} \\
 \diagdown \\
 2
 \end{array}
 \text{---}
 \begin{array}{c}
 \diagup \\
 \diagdown \\
 \text{---} 5 \\
 \diagup \\
 \diagdown \\
 6
 \end{array}
 . \tag{3.26}$$

The first diagram is flavour-ordered according to both the multiplet and singlet terms. The second diagram is also flavour-ordered according to our definitions, but gives the non-flavour-ordered structure  $\langle 234 \rangle \langle 561 \rangle$  under the singlet. The third diagram is not flavour-ordered, but the singlet gives the flavour-ordered structure  $\langle 123 \rangle \langle 456 \rangle$ . Since the only permutation contained in both  $\mathbb{Z}_{\{6\}}$  and  $\mathbb{Z}_{\{3,3\}}$  is id, the behaviour of the singlet and multiplet terms is clearly very different and must be treated carefully.

There is, however, an elegant solution. As stated previously, the singlet term in (3.15) is not present in  $U(N_f)$ . Therefore, in the  $U(N_f)$  NLSM we may always do flavour-ordering without singlet issues. We can extend this to  $SU(N_f)$  by using its similarity to  $U(N_f)$ .

The  $U(N_f)$  algebra differs from the  $SU(N_f)$  algebra by a non-traceless generator  $t^0$  that commutes with all other generators. Due to the latter property, its associated field  $\phi^0$  forms a  $U(1)$  singlet separate from the  $SU(N_f)$  multiplet  $\phi^a$ . With this in mind, a more elucidating form of (3.15) is

$$\sum_{a=1}^{N_f^2-1} \langle X t^a \rangle \langle t^a Y \rangle = \sum_{a=0}^{N_f^2-1} \langle X t^a \rangle \langle t^a Y \rangle - \langle X t^0 \rangle \langle t^0 Y \rangle, \quad (3.27)$$

where we temporarily suppress Einstein summation. This expression suggests that a  $SU(N_f)$  propagator (left) represents a  $U(N_f)$  propagator (right) minus the singlet propagator, and explains our naming of the terms in (3.15). The  $N_f^{-1}$  is absorbed into  $t^0$  since  $t^0 = \mathbb{1}/\sqrt{N_f}$ .

Now, if we extend our Lagrangian-building field like

$$\hat{\Phi}(\phi^0, \phi) = t^0 \phi^0 + \Phi(\phi), \quad \hat{u}(\phi^0, \phi) = \exp\left(\frac{i\hat{\Phi}}{F\sqrt{2}}\right) = \exp\left(\frac{i\phi^0 t^0}{F\sqrt{2}}\right) u(\phi), \quad (3.28)$$

where  $u(\phi) \in SU(N_f)$  and  $\hat{u}(\phi^0, \phi) \in U(N_f)$ , we see that

$$\hat{U} = \hat{u}^2 \quad \Rightarrow \quad \hat{U}^\dagger \partial_\mu \hat{U} = \left(\frac{i\sqrt{2}}{F\sqrt{N_f}}\right) \partial_\mu \phi^0 + U^\dagger \partial_\mu U \quad (3.29)$$

(remembering that  $U^\dagger \partial_\mu U$  is equivalent to  $u_\mu$ ), and therefore

$$\hat{\mathcal{L}}_2 = \frac{1}{2} \partial_\mu \phi^0 \partial^\mu \phi^0 + \frac{F^2}{4} \langle u_\mu u^\mu \rangle. \quad (3.30)$$

At this order, the singlet decouples from the other fields and forms a free theory. Therefore, no  $\mathcal{O}(p^2)$  vertex involves the singlet, so there is no distinction between  $U(N_f)$  and  $SU(N_f)$  amplitudes at this order, and we may ignore the singlet term in (3.15).

This observation was sufficient in [36], but we must handle the singlet problem beyond  $\mathcal{O}(p^2)$ .  $\mathcal{L}_4$  and all higher-order Lagrangians introduce vertices that couple the singlet to the other particles. However, a singlet propagator can only exist if both vertices at its ends couple to it. Since this requires at least two vertices of at least  $\mathcal{O}(p^4)$ , the diagram as a

whole must be at least  $\mathcal{O}(p^6)$  to include such complications.<sup>5,6</sup> Therefore, flavour-ordering at  $\mathcal{O}(p^4)$  works with no other complications than the introduction of split vertices.

At  $\mathcal{O}(p^6)$  and above, the singlet term in (3.15) can not be avoided in  $SU(N_f)$ , but the interpretation of (3.27) still holds. In order to build a  $SU(N_f)$  amplitude, we first work in  $U(N_f)$  to build flavour-ordered diagrams using only the multiplet term. Then, we construct all diagrams with singlet propagators in a similar fashion, maintaining flavour-ordering independently. For instance, the full suite of  $\mathcal{O}(p^6)$  6-point diagrams is

$$(3.31)$$

including one singlet propagator, indicated by a dashed line. It implicitly includes a factor of  $-N_f^{-1}$ , and its flavour structure is split  $\{3, 3\}$  over the propagator. All cyclings of the two traces should be counted as distinct, since the vertices are invariant under  $\mathbb{Z}_4$ , not  $\mathbb{Z}_3$ . By adding the singlet diagrams to the others, we get the stripped  $SU(N_f)$  amplitude.

The singlet diagram contains all contractions that are flavour-ordered under the singlet term, like the first and last diagram in (3.26). The decoupling of the singlet at  $\mathcal{O}(p^2)$  means that these contributions must cancel in the amplitude at this order, which is not at all obvious from the individual diagrams. Still, recasting the singlet terms as flavour-ordered singlet diagrams is valid, as follows from the uniqueness of the stripped amplitude.

### 3.6 Uniqueness of stripped amplitudes

Above, we have blindly trusted the definition of the stripped amplitude as everything that comes attached to the flavour-ordered structure  $\mathcal{F}_{\text{id}}(R)$ . If this definition is not unique, flavour-ordering would not necessarily be valid, and we could not rely on our use of singlet diagrams. However, we can show that the stripped amplitude is indeed unique, using a generalisation of a method presented by [44] and adapted to flavour-ordering by [36].

The uniqueness hinges on the orthogonality relation

$$\mathcal{F}_\sigma(Q) \cdot [\mathcal{F}_\rho(R)]^* = N_f^n \begin{cases} 1 + \mathcal{O}(N_f^{-2}) & \text{if } Q = R \text{ and } \sigma \equiv \rho \pmod{\mathbb{Z}_R}, \\ \mathcal{O}(N_f^{-\gamma}) & \text{otherwise } (\gamma \geq 1; \text{ see below}) \end{cases} \quad (3.32)$$

<sup>5</sup>If the singlet forms a loop, only one  $\mathcal{O}(p^4)$  vertex is necessary, but the loop itself increases the power counting, so  $\mathcal{O}(p^6)$  is needed in this case as well.

<sup>6</sup>An interesting parallel can be seen in [42], where  $U(1)$  gluons similar to our singlets must be introduced in perturbative QCD. While our singlets only emerge with at least two higher-order vertices, their  $U(1)$  gluons cancel unless the diagram contains at least two quark lines. In general, there are several intriguing analogies between the inclusion of quark lines in gluon scattering (where there are no higher-order vertices) and the inclusion of higher-order vertices in the NLSM (where there are no quark lines).

using the notation defined in section 3.1. The dot in the left-hand side indicates contraction over all flavour indices. If  $Q \neq R$ ,  $\gamma \geq 1$ , and if  $\sigma \not\equiv \rho \pmod{\mathbb{Z}_R}$ ,  $\gamma \geq 2$ ; therefore, the single-trace version (i.e. that given in [36]) has  $\mathcal{O}(N_f^{-2})$  as its second case. The more different the flavour structures are, the larger  $\gamma$  is. The relation (3.32) is proven in appendix B and states that any given flavour structure  $\mathcal{F}_\sigma(Q)$  is orthogonal at leading order in  $N_f$  to all other flavour structures whose permutations are not equivalent to  $\sigma$ , or whose flavour splittings are not equal to  $Q$ .

In the context of stripped amplitude uniqueness, (3.32) can be applied as follows. In analogy with (3.5) and (3.12), we write some arbitrary quantity  $\mathcal{X}$  in the form

$$\mathcal{X}^{a_1 \cdots a_n} = \sum_{R \in \mathcal{R}} \sum_{\sigma \in \mathcal{S}_n / \mathbb{Z}_R} \mathcal{F}_\sigma(R) \mathcal{X}_{\sigma, R}, \quad (3.33)$$

where  $\mathcal{R}$  is some appropriate selection of flavour splittings. Then, we use the orthogonality relation (3.32) to perform the projection

$$\mathcal{X}^{a_1 \cdots a_n} [\mathcal{F}_{\text{id}}(R)]^* = N_f^n \left[ \mathcal{X}_{\text{id}, R} + \mathcal{O}\left(\frac{1}{N_f}\right) \right]. \quad (3.34)$$

This means that we can always project out the stripped  $\mathcal{X}$ , and that any overlap with other terms must come suppressed by at least  $N_f^{-1}$ . In a stripped amplitude of  $\mathcal{O}(p^4)$  or lower, the stripped amplitude can not contain any powers of  $N_f^{-1}$  due to the decoupling of the singlet, so there can be no overlap for arbitrary  $N_f$ . This proves that stripped amplitudes are unique at  $\mathcal{O}(p^4)$  or below.

At higher orders, things are not as simple, since there are possibly many factors of  $N_f^{-1}$ . This would allow mixing between different stripped  $\mathcal{X}$ 's, threatening to break uniqueness. However, it can be resolved by expressing  $\mathcal{X}^{a_1 \cdots a_n}$  as a polynomial in  $N_f^{-1}$ ,

$$\mathcal{X}^{a_1 \cdots a_n} = \mathcal{X}_0^{a_1 \cdots a_n} + \frac{1}{N_f} \mathcal{X}_1^{a_1 \cdots a_n} + \frac{1}{N_f^2} \mathcal{X}_2^{a_1 \cdots a_n} + \dots \quad (3.35)$$

such that each  $\mathcal{X}_i^{a_1 \cdots a_n}$ , and therefore also its stripped counterpart, is independent of  $N_f^{-1}$ . We then apply the projection to each  $\mathcal{X}_i^{a_1 \cdots a_n}$  independently, and ignore the  $\mathcal{O}(N_f^{-1})$  completely. Thus, stripped amplitudes, vertex factors, and other analogous quantities are unique to all orders.<sup>7</sup>

The proof holds for general  $N_f$ , but for any specific  $N_f$ , there may be additional relations between the generators that break the uniqueness. The Cayley-Hamilton relations provide such relations for small  $N_f$ . However, we always assume that the relations have been “exhausted” by removing terms from the Lagrangian, so that they do not affect the uniqueness of stripped amplitudes.

This proof in this section has significant consequences. Most importantly, it guarantees the correctness of our method of flavour ordering with split traces and singlets: gathering

---

<sup>7</sup>This uniqueness is of course only up to a permutation in  $\mathbb{Z}_R$ , but since we sum over those in the definition of the stripped quantity, they are unique for our purposes.

all flavour-ordered pieces of the full amplitude is guaranteed to equal the unique stripped amplitude. Also, uniqueness allows many properties of the full amplitude to carry over to the stripped amplitude, as is discussed below.

A second consequence is worthy of note. The full amplitude of some  $\mathcal{O}(p^N)$   $n$ -particle process is constructed from  $|\mathcal{R}(N, n)|$  different stripped amplitudes. When summed over permutations according to (3.12), the total number of flavour structures grows to

$$\mathcal{N}_{N,n} \sim \sum_{R \in \mathcal{R}(N,n)} \frac{|\mathcal{S}_n|}{|\mathbb{Z}_R|}, \quad (3.36)$$

which is a very rapidly growing number — even at  $\mathcal{O}(p^2)$ ,  $\mathcal{N}(2, n) \sim (n-1)!$ . Since the flavour structures are not truly orthogonal, the expression for the cross section of the process, proportional to  $\mathcal{M}_{N,n}^{a_1 \dots a_n} [\mathcal{M}_{N,n}^{a_1 \dots a_n}]^\dagger$ , grows in length as  $(\mathcal{N}_{N,n})^2$ . However, the expression for the cross section contracts the flavour structures as in (3.32), which suppresses products of non-equivalent flavour structures by a factor of  $N_f^{-1}$  for each difference (or  $N_f^{-2}$  in the single-trace case). Therefore, in the limit  $N_f \rightarrow \infty$ , flavour structures *are* orthogonal, and the cross section only grows as  $\mathcal{N}_{N,n}$ . Even with finite  $N_f$ , most cross-terms will be heavily suppressed, and can most likely be ignored.

An alternative approach would be to construct other bases for flavour space that are more orthogonal than the trace bases used here, as is done in perturbative QCD by [45]. Such methods have so far not been applied in the present context.

## 4 NLSM amplitudes

In this section, we introduce and generalise several concepts related to NLSM amplitudes and flavour-ordering.

### 4.1 Adler zeroes and soft limits

In any effective field theory emerging from the spontaneous breaking of a global symmetry, the amplitude possesses the so-called Adler zero,

$$\lim_{\varepsilon \rightarrow 0} \mathcal{M}^{a_1 \dots a_n}(p_1, \dots, \varepsilon p_i, \dots, p_n) = 0, \quad (4.1)$$

for any  $i$  [12, 46]. The approach to zero will generally go as  $\varepsilon^\sigma$ , where the *soft degree*  $\sigma \geq 1$  can be used to classify and construct EFTs [13, 47]. The NLSM has  $\sigma = 1$ . Due to the orthogonality of flavour structures and the uniqueness of stripped amplitudes, Adler zeroes may only exist in the full amplitude if they also exist, with the same soft degree, in the stripped amplitudes. Therefore, (4.1) and any statement relying on it can equally well be applied to the stripped amplitudes.

The Adler zeroes may be used as a starting point to construct amplitudes through recursion relations [11, 15]. For our purposes, however, their main use is in validating the correctness of complicated stripped amplitudes. Since far from every term in the amplitude is proportional to  $p_i$ , the Adler zero must manifest itself through intricate cancellations.

Therefore, any error in the amplitude is extremely likely to give a finite right-hand side in (4.1).

Beside the Adler zeroes, there also exists the *double soft limit*, where two momenta are sent to zero at the same rate. It turns out that the double soft limit of any  $(n+2)$ -particle amplitude can be expressed in terms of  $n$ -particle amplitudes with the soft particles removed; for the NLSM, the specific form is

$$\lim_{\varepsilon \rightarrow 0} \mathcal{M}_{m,n+2}^{aba_1 \dots a_n}(\varepsilon p, \varepsilon q, p_1, \dots, p_n) = -\frac{1}{4F^2} \sum_{i=1}^n f^{abc} f^{a_i dc} \frac{p_i \cdot (p-q)}{p_i \cdot (p+q)} \mathcal{M}_{m,n}^{a_1 \dots a_{(i-1)} da_{(i+1)} \dots a_n}(p_1, \dots, p_n). \quad (4.2)$$

This was conjectured in [48] and proven in [36]. Like the Adler zero, it can be projected to a relation for stripped amplitudes, although the projection is not entirely trivial. The result for single-trace flavour structures is given in [36]. We derive the counterpart for general flavour structures in appendix C, with the result being as follows. At any order  $m$  in the power counting and for any flavour split  $R \in \mathcal{R}(m, n+2)$ , the double soft limit

$$\lim_{\varepsilon \rightarrow 0} \mathcal{M}_{m,R}(p_1, \dots, p_{i-1}, \varepsilon p_i, \dots, \varepsilon p_j, p_{j+1}, \dots, p_{n+2}) \quad (4.3)$$

is nonzero if the indices  $i-1$ ,  $i$ ,  $j$  and  $j+1$  are consecutive and lie within the same trace; we will call this condition  $\mathcal{C}$ . It is also nonzero if the indices can be made to satisfy  $\mathcal{C}$  by applying a permutation in  $\mathbb{Z}_R$  and possibly swapping  $i$  and  $j$ . In all other cases, the double soft limit is zero.

Since  $\mathcal{M}_{m,R}$  is invariant under  $\mathbb{Z}_R$ , we can without loss of generality assume that  $\mathcal{C}$  holds whenever the double soft limit is nonzero. Assuming this, the double soft limit is

$$\begin{aligned} & \lim_{\varepsilon \rightarrow 0} \mathcal{M}_{m,R}(p_1, \dots, \varepsilon p_i, \varepsilon p_j, \dots, p_{(n+2)}) \\ &= \frac{1}{4F^2} \left( \frac{p_{(j+1)} \cdot (p_i - p_j)}{p_{(j+1)} \cdot (p_i + p_j)} - \frac{p_{(i-1)} \cdot (p_i - p_j)}{p_{(i-1)} \cdot (p_i + p_j)} \right) \mathcal{M}_{m,R'}(p_1, \dots, p_{(i-1)}, p_{(j+1)}, \dots, p_{(n+2)}), \end{aligned} \quad (4.4)$$

where  $R' \in \mathcal{R}(m, n)$  is  $R$  with the location of the soft particles removed and  $j = i+1$ . The result, which generalises that given in [36], is quite remarkable: for properly chosen  $i, j$ , the double soft limit amounts to removing the soft particles from the amplitude and multiplying by a simple kinetic factor. The factor is similar to those that arise in IR divergences, which is understandable — both arise from propagators going on-shell in the soft (IR) limit.

## 4.2 Generalised Mandelstam invariants

In order to express stripped amplitudes in a way that naturally includes on-shellness and conservation of momentum, we will employ bases of generalised Mandelstam invariants in

the form

$$s_{ijk\dots} = (p_i + p_j + p_k + \dots)^2, \quad (4.5)$$

In this notation, the standard 4-particle Mandelstam invariants are

$$s = s_{12} = s_{34}, \quad t = s_{13} = s_{24}, \quad u = s_{23} = s_{41}. \quad (4.6)$$

Since  $s + t + u = 0$ , this basis is overcomplete, and one element can be removed. We will generally use bases where  $ijk\dots$  are consecutive, so we choose to keep  $\{s, u\}$  as the 4-particle basis.

For  $n$  particles, the products of momenta are related to the invariants with consecutive indices through

$$\begin{aligned} 2p_i \cdot p_{i+1} &= s_{i(i+1)}, \\ 2p_i \cdot p_{i+2} &= s_{i(i+1)(i+2)} - s_{i(i+1)} - s_{(i+1)(i+2)}, \\ j > i + 2: \quad 2p_i \cdot p_j &= s_{i\dots j} - s_{i\dots(j-1)} - s_{(i+1)\dots j} + s_{(i+1)\dots(j-1)}. \end{aligned} \quad (4.7)$$

Based on this, a complete basis of invariants for  $n = 6$  is

$$\mathcal{B}_{\{6\}} = \{s_{12}, s_{23}, s_{34}, s_{45}, s_{56}, s_{61}, s_{123}, s_{234}, s_{345}\}, \quad (4.8)$$

where  $s_{456}$  etc. are not needed due to conservation of momentum in the form

$$s_{i\dots(i+k-1)} = s_{(i+k)\dots(i-1)}, \quad (4.9)$$

with indices cycling around from  $n$  to 1. The form of  $\mathcal{B}_{\{6\}}$  can be carried on to any even  $n$ , giving

$$\mathcal{B}_{\{n\}} = \{s_{12}, s_{23}, \dots, s_{n(n-1)}, s_{n1}, s_{123}, s_{234}, \dots, s_{n12}, \dots, s_{12\dots(n/2)}, \dots, s_{(n/2-1)\dots(n-1)}\}. \quad (4.10)$$

This contains  $n(n-3)/2$  invariants, which is also the number of independent products that can be formed from  $\{p_1, \dots, p_n\}$  with all  $p_i^2 = 0$ .<sup>8</sup> Note that all invariants have consecutive indices.

These bases are only linearly independent in sufficiently high spacetime dimensions  $D$ . If  $D < n + 1$ , the Gram determinant gives relations among the basis elements. In practice, these relations are so algebraically messy that we have found it simpler to always work in arbitrary  $D$ .

Mandelstam invariants have further benefits beyond taking care of on-shellness and conservation of momentum. In an  $n$ -point  $\mathcal{O}(p^2)$  single trace flavour-ordered tree diagram, all propagators carry a momentum  $q$  such that  $q^2 \in \mathcal{B}_{\{n\}}$ . Therefore,  $\mathcal{O}(p^2)$  stripped amplitudes will never contain a denominator with a sum of several invariants, making their

---

<sup>8</sup>There are  $n(n+1)/2$  ways to form products of pairs of  $p_i$ ,  $i \in \{1, \dots, n\}$ . Of these,  $n$  vanish due to  $p_i^2 = 0$ . Conservation of momentum implies that  $p_n = \sum_{i=1}^{n-1} p_i$ , which gives  $n$  linear combinations among the remaining products, reducing the number of independent ones to  $n(n+1)/2 - 2n = n(n-3)/2$ .

algebraic handling simpler. This is not true for diagrams with multi-trace flavour structures. It is also not possible to find a different basis that contains all squared propagator momenta in the general case; for instance, the set of all possible  $q^2$  under  $R = \{2, 6\}$  is not linearly independent.

Another use of Mandelstam invariants is the shortening of stripped amplitudes. As a consequence of invariance under  $\mathbb{Z}_R$ , any stripped amplitude can be written in the form

$$\mathcal{M}_{m,R}(p_1, \dots, p_n) = (\text{simpler expression}) + [\mathbb{Z}_R], \quad (4.11)$$

where we use a shorthand for the sum over  $\mathbb{Z}_R$ , generalising the familiar idiom “+cycl.”. The simpler expression is rather obvious for simple amplitudes, but for more complicated cases, it is an enormous aid to readability.

Any stripped amplitude can be simplified as above by separating it into simple terms, separating the terms into cosets under  $\mathbb{Z}_R$ , and picking a single representative from each coset. The “simpler expression” in (4.11) will then be the sum of the representatives. For  $R = \{n\}$ , this works because for any  $s_{ij\dots} \in \mathcal{B}_{\{n\}}$  and  $\sigma \in \mathbb{Z}_{\{n\}}$ , applying  $\sigma$  to the indices of  $s_{ij\dots}$  yields another element in  $\mathcal{B}_{\{n\}}$ . Thus,  $\mathcal{B}_{\{n\}}$  can be said to be *closed* under  $\mathbb{Z}_{\{n\}}$ . However, the basis given in (4.10) is not closed under any  $\mathbb{Z}_R$  with  $R \neq \{n\}$  (with the sole exception of  $R = \{2, 2\}$ ), so the separation into cosets fails. Simplifying general amplitudes therefore requires either painstaking manual work, or a Mandelstam basis that is closed under  $\mathbb{Z}_R$ . We have no general method of finding such bases. In appendix D, we present closed bases for  $\mathbb{Z}_{\{2,4\}}$ ,  $\mathbb{Z}_{\{3,3\}}$  and  $\mathbb{Z}_{\{2,2,2\}}$ . These cover all flavour structures that appear for  $n \leq 6$ .

### 4.3 Diagram generation

For most amplitudes presented here, the number of diagrams is small enough that they are easily found by hand, but above a dozen or so diagrams, this becomes a slow and error-prone process. We therefore automated the process by designing a program called FODGE (Flavour-Ordered Diagram Generator) written in C++.<sup>9</sup> It produces TikZ code for drawing the diagrams, and generates the input to a set of FORM procedures that compute the amplitudes.<sup>10</sup> The same procedures were used with manual input for computing simpler amplitudes. Inspiration was taken from the diagram generator used in [51, 52].

The diagram generation works recursively. A list of all  $\mathcal{O}(p^M)$   $N$ -point diagrams can be generated by generating all  $\mathcal{O}(p^m)$   $n$ -point diagrams for  $m \leq M$  and  $n \leq N - 2$ , and then listing all ways to attach a  $\mathcal{O}(p^{2+M-m})$   $(2 + N - n)$ -point vertex to their external legs. Adding a list of  $\mathcal{O}(p^M)$   $N$ -point single-vertex diagram and removing duplicates completes the list. The number of duplicates can be reduced by restricting  $m$  and  $n$ .

The number of independent labellings on each diagram must then be determined. Representing diagrams in a way that shows their symmetries turns out to be very difficult when complicated flavour structures are involved. This was not entirely successfully tried

<sup>9</sup>The source code of FODGE can be found at <https://github.com/mssjo/fodge>.

<sup>10</sup>The FORM procedures can be found at <https://github.com/mssjo/flavour-order>. For FORM itself, see [49, 50].

in the original FODGE used in [37]. Here, we take a different approach: each diagram is associated with all flavour-ordered labellings of its external legs that give unique kinematic structures. This removes the need to explicitly consider its symmetries; internally, the diagrams can be represented in whatever way is convenient.

As is pointed out below (3.17), a kinematic structure is uniquely determined by the propagator momenta it contains. It is easy to see that this holds for any  $\mathcal{O}(p^2)$  diagram. At higher orders, it is sufficient to add the order of the vertices at the ends of each propagator. The flavour splits of the vertices are not needed if the overall flavour split of the diagram is provided. For singlet diagrams, we must also specify how the vertex is cycled relative to the singlet propagator, by writing down the momentum carried by a vertex leg adjacent to the propagator. In general, any kinematic factor is uniquely determined by listing all vertices and the momenta carried by their legs, but this can be shown to reduce to these simpler rules when diagrams are flavour-ordered.

Thus, FODGE generates all diagrams of a given order and size, equips each diagram with an arbitrary flavour-ordered labelling, and determines the kinematic factor as described above.  $\mathbb{Z}_R$  is then applied to generate all other labellings, but only a subset that gives distinct kinematic factors is kept. If the choice of subset is consistent, equivalent diagrams will always give an identical list of kinematic factors, so duplicates are easily removed.

Knowing the labellings also makes the diagram generation more efficient. There is no need to attach a vertex to several legs that are equivalent to each other under the symmetries. By dividing the set of labels into cosets under  $\mathbb{Z}_R$ , it is sufficient to attach vertices to legs that, in one of the distinct labellings, carries a coset representative as its label. This reduces the number of generated duplicates.

## 5 Explicit amplitudes

Using the methods developed in the previous sections, we have computed several stripped NLSM amplitudes, several of which have not previously been determined. These we discuss in this section.

### 5.1 4-point amplitudes

These amplitudes are by far the simplest, since their tree-level diagrams contain no propagators and only carry two flavour structures ( $\{4\}$  and  $\{2, 2\}$ ), or only one in the  $\mathcal{O}(p^2)$  case. At  $\mathcal{O}(p^6)$  and above, they only receive contributions from the Lagrangian terms with no more than four  $u_\mu$ 's, which is a tiny subset of the total Lagrangian.

The  $\mathcal{O}(p^2)$  4-point amplitude is given by a single diagram and a simple stripped amplitude,

$$\begin{array}{c} \diagup \\ \times \\ \diagdown \end{array} \quad -iF^2 \mathcal{M}_{2,\{4\}} = \frac{t}{2}, \quad (5.1)$$

where  $t$  is the Mandelstam invariant  $(p_1 + p_3)^2$ . We have pulled factors of  $i$  and  $F$  over to the left-hand side for clarity. The only independent  $\mathcal{O}(p^2)$  kinematic structure that is invariant under  $\mathbb{Z}_{\{4\}}$  is  $t$ , so the form of the right-hand side could have been guessed based on symmetry.

If we plug (5.1) into (3.12) and apply some  $SU(2)$  group algebra, we recover the familiar  $N_f = 2$  amplitude

$$\mathcal{M}_{2,4}^{abcd}(s, t, u) = \frac{-4i}{F^2} \left[ s\delta^{ab}\delta^{cd} + t\delta^{ac}\delta^{bd} + u\delta^{ad}\delta^{bc} \right] \quad (5.2)$$

with the Mandelstam invariants defined as in section 4.2.

The  $\mathcal{O}(p^4)$  4-point amplitude consists of the two diagrams

$$\begin{array}{c} \text{Diagram 1: } \begin{array}{c} \diagup \quad \diagdown \\ \diagdown \quad \diagup \end{array} \quad -iF^4 \mathcal{M}_{4,\{4\}} = 2L_3(u^2 + s^2) + 4L_0 t^2, \end{array} \quad (5.3)$$

$$\begin{array}{c} \text{Diagram 2: } \begin{array}{c} \diagdown \quad \diagup \\ \diagup \quad \diagdown \end{array} \quad -iF^4 \mathcal{M}_{4,\{2,2\}} = 8L_1 s^2 + 4L_2(t^2 + u^2), \end{array} \quad (5.4)$$

which includes the simplest example of a flavour split. There are now two independent  $\mathbb{Z}_4$ -invariant kinematic structures,  $t^2$  and  $s^2 + u^2$ , and likewise two independent  $\mathbb{Z}_{\{2,2\}}$ -invariant ones,  $s^2$  and  $t^2 + u^2$ . All four appear equipped with one LEC each. The full amplitude is analogous to (5.2), but with various linear combinations of the LECs and Mandelstam variables in place of  $s$ ,  $t$  and  $u$ . The full amplitude agrees with the known results, see [7] and references therein.

The  $\mathcal{O}(p^6)$  4-point amplitude, like its  $\mathcal{O}(p^4)$  analogue, has two diagrams,

$$\begin{array}{c} \text{Diagram 1: } \begin{array}{c} \diagup \quad \diagdown \\ \diagdown \quad \diagup \end{array} \quad -iF^4 \mathcal{M}_{6,\{4\}} = -L_{6,3}t(s^2 + u^2) - 2L_{6,4}t^3, \end{array} \quad (5.5)$$

$$\begin{array}{c} \text{Diagram 2: } \begin{array}{c} \diagdown \quad \diagup \\ \diagup \quad \diagdown \end{array} \quad -iF^4 \mathcal{M}_{6,\{2,2\}} = -2L_{6,1}(t^3 + u^3) + \frac{2}{3}L_{6,2}(s^3 + t^3 + u^3). \end{array} \quad (5.6)$$

As for  $\mathcal{O}(p^4)$ , there are two independent  $\mathbb{Z}_4$ -invariant kinematic structures,  $t^3$  and  $t(s^2 + u^2)$ , and two independent  $\mathbb{Z}_{\{2,2\}}$ -invariant ones,  $s^3$  and  $s(t^2 + u^2)$ . These four correspond to the four LECs —  $s^3 + t^3 + u^3$  is a linear combination of  $s^3$  and  $s(t^2 + u^2)$ . The full amplitude agrees with the result in [7].

The  $\mathcal{O}(p^8)$  amplitude, like its lower-order analogues, has two diagrams,

$$\begin{array}{c} \text{Diagram 1: } \begin{array}{c} \diagup \quad \diagdown \\ \diagdown \quad \diagup \end{array} \quad -iF^4 \mathcal{M}_{8,\{4\}} = L_{8,4}s^2u^2 + \frac{1}{2}L_{8,5}t^2(s^2 + u^2) + L_{8,6}t^4, \end{array} \quad (5.7)$$

$$\begin{array}{c} \text{Diagram 2: } \begin{array}{c} \diagdown \quad \diagup \\ \diagup \quad \diagdown \end{array} \quad -iF^4 \mathcal{M}_{8,\{2,2\}} = L_{8,1}s^2(t^2 + u^2) + L_{8,2}(t^4 + u^4) + 2L_{8,3}t^2u^2, \end{array} \quad (5.8)$$

There are now three independent  $\mathbb{Z}_4$ -invariant kinematic structures,  $t^4$ ,  $t^2(s^2 + u^2)$  and  $s^2u^2$ , and correspondingly three for  $\mathbb{Z}_{\{2,2\}}$ . This is reflected in the six LECs.

Similarly,  $\mathcal{M}_{10,\{4\}}$  will be a linear combination of  $s^5$ ,  $s^3tu$  and  $st^2u^2$ , and  $\mathcal{M}_{10,\{2,2\}}$  will be a linear combination of  $t^5$ ,  $t^3us$  and  $tu^2s^2$ , since these are the only independent  $\mathcal{O}(p^{10})$  kinematic structures that are invariant under  $\mathbb{Z}_{\{4\}}$  and  $\mathbb{Z}_{\{2,2\}}$ , respectively. The coefficients will be linear combinations of the LECs of the terms in  $\mathcal{L}_{10}$  that only contain

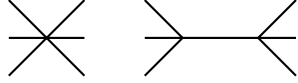
four  $u_\mu$ 's. These terms, along with the rest of  $\mathcal{L}_{10}$ , have not yet been studied. The same pattern can be applied to  $\mathcal{O}(p^{12})$  and beyond.

Note that the above discussion is fully compatible with section 5 in [41] where we have two functions with properties  $B(s, t, u) = B(u, t, s)$  and  $C(s, t, u) = C(s, u, t)$ . Independent combinations in  $B$  at order  $p^{2n}$  are made from  $t^{n-2i}(s-u)^{2i}$  and in  $C$  from  $s^{n-2i}(t-u)^{2i}$ .

## 5.2 The $\mathcal{O}(p^2)$ 6- and 8-point amplitudes

The leading order in the power counting offers a relatively simple playground for flavour-ordering, free from splittings and singlets. It is relatively well explored, and the amplitudes presented here were also calculated in [36] using different methods.

The 6-point amplitude is given by the diagrams


(5.9)

Each diagram represents the sum of all distinct labellings of its legs, as described in section 3. The amplitude is

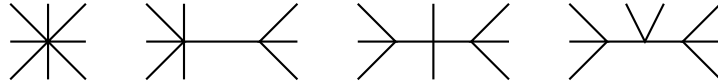
$$\begin{aligned}
 -4iF^4 \mathcal{M}_{2,6} = & s_{12} + s_{23} + s_{34} + s_{45} + s_{56} + s_{61} \\
 & - \frac{(s_{12} + s_{23})(s_{45} + s_{56})}{s_{123}} - \frac{(s_{23} + s_{34})(s_{56} + s_{61})}{s_{234}} - \frac{(s_{34} + s_{45})(s_{61} + s_{12})}{s_{345}},
 \end{aligned} \tag{5.10}$$

which suggests the simplified form as defined in (4.11)

$$-4iF^4 \mathcal{M}_{2,6} = \left\{ s_{12} - \frac{1}{2} \frac{(s_{12} + s_{23})(s_{45} + s_{56})}{s_{123}} \right\} + [\mathbb{Z}_6], \tag{5.11}$$

where  $[\mathbb{Z}_6]$  indicates summation over all cyclic permutations. Note the factor of  $1/2$ , which expresses that the second term has twofold symmetry under rotation, a trait that is shared by the second diagram above.

The 8-point amplitude is given by the diagrams


(5.12)

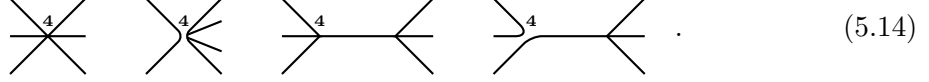
and its stripped amplitude is, in a similarly simplified form,

$$\begin{aligned}
 -8iF^6 \mathcal{M}_{2,8} = & \left\{ \frac{4s_{12} + s_{1234}}{2} - \frac{(s_{12} + s_{23})(s_{45} + s_{56} + s_{67} + s_{78} + s_{4567} + s_{5678})}{s_{123}} \right. \\
 & + \frac{1}{2} \frac{(s_{12} + s_{23})(s_{1234} + s_{4567})(s_{56} + s_{67})}{s_{123}s_{567}} \\
 & \left. + \frac{(s_{12} + s_{23})(s_{1234} + s_{45})(s_{67} + s_{78})}{s_{123}s_{678}} \right\} + [\mathbb{Z}_8]. \tag{5.13}
 \end{aligned}$$

The analogous 10- and 12-point amplitudes, the second of which has not been determined before, are presented in appendices E.2 and E.3.

### 5.3 The $\mathcal{O}(p^4)$ 6-point amplitude

The calculation of this amplitude hinges decisively on the use of split-trace flavour ordering. It was arrived at independently in a different form by [15] using recursion relations. Our result agrees with theirs. The amplitude is given by the four diagrams



Note that unlike its  $\mathcal{O}(p^2)$  counterpart, the third diagram is not symmetric due to the asymmetric placement of vertices. The amplitude has a single-trace and a two-trace part. The single-trace stripped amplitude is

$$\begin{aligned}
-iF^6 \mathcal{M}_{4,\{6\}} &= L_3 \left\{ s_{12} (s_{12} + s_{34} + s_{45}) - \frac{(s_{12} + s_{23})(s_{45}^2 + s_{56}^2)}{s_{123}} \right\} + [\mathbb{Z}_6] \\
&+ 2L_0 \left\{ s_{12} (s_{12} + s_{34} + 2s_{45}) + s_{123} (s_{612} - s_{61}) - \frac{(s_{12} + s_{23})(s_{45} + s_{56})^2}{s_{123}} \right\} + [\mathbb{Z}_6]
\end{aligned} \tag{5.15}$$

In order to find the simplified form of the two-trace part, it is extremely helpful to have a closed Mandelstam basis. In terms of the closed basis  $\mathcal{B}_{\{2,4\}} = \{t_1, \dots, t_9\}$  of (D.1), it is

$$\begin{aligned}
-iF^6 \mathcal{M}_{4,\{2,4\}} &= \frac{L_1}{2} \left\{ t_1 [t_1 + 2t_2 + t_3 - 3t_5] + \frac{(t_2 + t_3 + t_4)^2 [t_3 - 2t_5]}{2t_1} \right\} + [\mathbb{Z}_{\{2,4\}}] \\
&+ \frac{L_2}{8} \left\{ t_1 \left[ t_1 + 2t_2 + \frac{t_3}{2} - 3t_5 \right] + 4t_7^2 - 2t_9^2 \right. \\
&\left. + \frac{[(t_2 + t_3 + t_4)^2 + 4(t_7 + t_8 + t_9)^2] [t_3 - 2t_5]}{2t_1} \right\} + [\mathbb{Z}_{\{2,4\}}].
\end{aligned} \tag{5.16}$$

Note that the summation over cyclic permutations is replaced by summation over  $\mathbb{Z}_{\{2,4\}}$ .

### 5.4 Further amplitudes

We have computed the  $\mathcal{O}(p^6)$  6-point amplitude, and using the closed Mandelstam bases presented in appendix D, it is possible to present its reduced form given in appendix E.1. The  $\mathcal{O}(p^6)$  divergent part is given explicitly in the supplementary material [38] as well as the  $\mathcal{O}(p^8)$  expression. The  $\mathcal{O}(p^2)$  10-point is given in appendix E.2. Finally the  $\mathcal{O}(p^2)$  12-point amplitudes is given in appendix E.3.

We have also computed several amplitudes whose expressions are too large to overview. They have been verified by checking their Adler zeroes, and in some cases by running brute-force Feynman diagram calculations. Beyond these amplitudes, we have generated the

flavour-ordered diagrams of many more amplitudes using our program FODGE, described in section 4.3. Here, we only summarise the number and general properties of the diagrams to give an idea of how the complexity scales. The summary is given in table 1.

For all entries labelled “Yes” in table 1 that are not included in the main text, the flavour-ordered diagrams are given in the supplementary material [38]. Most of the amplitudes themselves are too long to be practically written down, but they can be generated by using the freely available programs described in section 4.3.

$\mathcal{O}(p^N)$	$n$	Number of diagrams						Computed?
		$SU(N_f)$	$U(N_f)$	$SU(3)$	$U(3)$	$SU(2)$	$U(2)$	
$\mathcal{O}(p^2)$	4	1						Yes (5.1)
	6	2						Yes (5.11)
	8	4						Yes (5.13)
	10	16						Yes (E.10)
	12	73						Yes* (E.11)
	14	414						No
$\mathcal{O}(p^4)$	4	2				1	1	Yes (5.4)
	6	4				2	2	Yes†* (5.15-5.16)
	8	18				8	8	Yes†* (E.2-E.9)
	10	90				43	43	Yes*
	12	577				283	283	No
$\mathcal{O}(p^6)$	4	2	2	2	2	1	1	Yes (5.6)
	6	10	9	9	8	4	3	Yes†*
	8	50	45	48	43	18	14	Yes*
	10	360	318	348	316	129	98	No
$\mathcal{O}(p^8)$	4	2	2	2	2	1	1	Yes* (5.8)
	6	11	10	10	9	4	3	Yes*
	8	105	85	97	77	34	21	No

**Table 1.** Summary of the number of  $\mathcal{O}(p^N)$   $n$ -point diagrams. The  $SU(N_f)$  column shows the general count, and the  $U(N_f)$  column shows the count without singlet diagrams. The  $SU(3)$  and  $SU(2)$  columns show the number of distinct diagrams left when some Lagrangian terms have been eliminated using the Cayley-Hamilton relation as discussed in section 2.1. Note that the distinction for  $N_f = 2$  assumes we remove the  $L_1$  and  $L_2$  term and emerges first at  $\mathcal{O}(p^4)$ . For  $N_f = 3$  it emerges first at  $\mathcal{O}(p^6)$ . The distinction between  $SU$  and  $U$  also emerges first at  $\mathcal{O}(p^6)$ . The rightmost column states whether an amplitude has been computed by us, and provides references to the explicit amplitudes when possible. Amplitudes marked with an asterisk have to our knowledge not been calculated before; the  $\mathcal{O}(p^4)$  6-point amplitude was recently independently reproduced by [15]. Amplitudes marked with a dagger have been verified with a brute-force Feynman diagram calculation; the remainder rely only on Adler zeroes for verification.

In the table, we note that the number of diagrams grows more rapidly with  $n$  (the number of particles) than with  $N$  (the power-counting order). Especially when  $N > n$ , the number of new diagrams is very small. This is also reflected in the computational effort needed: the  $\mathcal{O}(p^2)$  10-point,  $\mathcal{O}(p^6)$  8-point and  $\mathcal{O}(p^8)$  6-point amplitudes took approximately 10 minutes each to calculate with FORM [49, 50], while the  $\mathcal{O}(p^4)$  10-point amplitude took almost an hour and the  $\mathcal{O}(p^2)$  12-point amplitude took over 2 days. At high  $N$ ,

the calculation of vertex factors takes significant time, while at high  $n$ , the conversion to Mandelstam variables is very time-consuming due to the large dimension of the kinematic space.

As the table shows, we have calculated all amplitudes with less than 100 diagrams, excluding  $N \geq 10$ , where the Lagrangian is not yet known. If we decide to push the frontier of large  $n$  further in the future, we expect the required computational effort to be severe.

## 6 Conclusions

In this work we have extended flavour ordering methods to include multiple traces and higher orders in derivatives. The uniqueness of the method relies on the extended orthogonality relation (3.32). We implemented the constraints in a diagram generator and used this then to calculate a number of amplitudes in the NLSM with more legs and derivatives than obtained previously.

Our methods are fairly constrained in which models they can be applied to, since they hinge on the existence of flavour structures and the contraction identity (3.15). On the other hand, they are readily extended to extremely high-order and many-particle amplitudes. They may also have some applicability to loop diagrams and massive particles under  $\chi$ PT. A tentative discussion of these possibilities can be found in [37].

Flavour-ordering serves as an enhancement of the standard diagrammatic approach, and as such is rather brute-force in nature. This contrasts with the recursive approach developed in [11], in which subtler properties such as soft limits play a much clearer role. These methods can also be applied to a wider range of models. The downside is that practical calculations require algebraic manipulations that are not entirely obvious. Flavour-ordering calculations can be very extensive, but are mathematically trivial and easily automated. Further developments of recursion relations in [15] have offset the algebraic difficulties, but soft recursion retains the fundamental limitation that recursive calculation of an  $\mathcal{O}(p^m)$   $n$ -point amplitude requires  $n > m$ . Therefore, the  $\mathcal{O}(p^6)$  6-point can not be reached by such means, and must be supplied as a seed amplitude if  $\mathcal{O}(p^6)$  amplitudes are to be calculated for more than 6 particles. For this, our methods seem to be the only viable option other than brute-force Feynman diagrams.

## Acknowledgements

We thank Malin Sjö Dahl for correcting an earlier version of (3.32). KK enjoyed kind hospitality at Lund University while most of this work was realized. This work is supported in part by the Swedish Research Council grants contract numbers 2015-04089 and 2016-05996, by the European Research Council (ERC) under the European Union’s Horizon 2020 research and innovation programme under grant agreement No 668679, and the Czech Government projects GACR 18-17224S and LTAUSA17069.

## A The NNLO NLSM Lagrangian

The NNLO  $\chi$ PT Lagrangian  $\mathcal{L}_6^{\chi\text{PT}}$  was first determined in [40]. It has 21 terms that do not vanish when external fields are removed, but this turns out to be an overcomplete basis for the NLSM. In tandem with the NNNLO  $\chi$ PT Lagrangian  $\mathcal{L}_8$  in [41], the authors of that paper produced a version of  $\mathcal{L}_6^{\chi\text{PT}}$  where removing external fields yields a *minimal* NLSM Lagrangian with 19 terms. It was not published there, but we present it in table 2. The first 135 terms of the Lagrangian in [41] constitute a minimal NLSM Lagrangian  $\mathcal{L}_8$ .

The Lagrangian of [40] is expressed as

$$\mathcal{L}_6^{\chi\text{PT}} = \sum_{i=1}^{112} K_i Y_i, \quad (\text{A.1})$$

where  $K_i$  are LECs and  $Y_i$  are monomials in the fields. Terms 1–6 and 49–63 remain when external fields are removed. All monomials except  $Y_1$ ,  $Y_2$  and  $Y_6$  correspond directly to monomials in the minimal NLSM Lagrangian

$$\mathcal{L}_6 = \sum_{i=1}^{19} L_{6,i} \mathcal{O}_{6,i}, \quad (\text{A.2})$$

where  $L_{6,i}$  are LECs and  $\mathcal{O}_{6,i}$  are monomials. The remaining  $Y_i$  can be decomposed in terms of  $\mathcal{O}_{6,i}$  using the relations described in [41], which for the NLSM simplify to

$$\begin{aligned} \nabla_\mu u_\nu &= \nabla_\nu u_\mu, & \nabla_\mu u^\mu &= 0, \\ [\nabla_\mu, \nabla_\nu] u_\rho &= \frac{1}{4} [[u_\mu, u_\nu], u_\rho]. \end{aligned} \quad (\text{A.3})$$

This yields the relations

$$Y_1 = -3\mathcal{O}_{6,3} + \mathcal{O}_{6,4} + \mathcal{O}_{6,15} - 2\mathcal{O}_{6,16} + \frac{1}{2}\mathcal{O}_{6,17} + \mathcal{O}_{6,18} - \frac{1}{2}\mathcal{O}_{6,19}, \quad (\text{A.4})$$

$$Y_2 = -8\mathcal{O}_{6,2} + 2\mathcal{O}_{6,8} - 2\mathcal{O}_{6,9}, \quad (\text{A.5})$$

$$Y_6 = 4\frac{\mathcal{O}_{6,2} - \mathcal{O}_{6,1}}{3} - 2\frac{\mathcal{O}_{6,9} - \mathcal{O}_{6,8}}{3} - 2\frac{\mathcal{O}_{6,12} - \mathcal{O}_{6,11}}{3}. \quad (\text{A.6})$$

Furthermore, some factors of 2 appear since [40] includes higher derivatives in terms of  $h_{\mu\nu} \equiv \nabla_\mu u_\nu + \nabla_\nu u_\mu$ , which is just  $2\nabla_\mu u_\nu$  in the NLSM.

### A.1 Renormalisation

NNLO  $\chi$ PT was renormalised in [53], based on [40]. For renormalisation in the NLSM, we transfer those results to the minimal Lagrangian given in table 2. For details on the renormalisation, see [53] and sources therein. At NLO, it is performed by splitting the LECs as

$$L_i = (c\mu)^{d-4} [L_i^r(\mu, d) + \Gamma_i \Lambda], \quad \Lambda = \frac{1}{16\pi^2(d-4)}. \quad (\text{A.7})$$

Monomial	Number in $\mathcal{L}_6$			Relation to [40]
	$SU(N_f)$	$SU(3)$	$SU(2)$	
$\langle u_\mu \nabla_\nu u_\rho \rangle \langle u^\mu \nabla^\nu u^\rho \rangle$	1	1	1	$K_4 - \frac{4}{3}K_6$
$\langle u_\mu \nabla_\nu u_\rho \rangle \langle u^\rho \nabla^\mu u^\nu \rangle$	2	2		$-8K_2 + \frac{4}{3}K_6$
$\langle u_\mu \nabla_\nu u^\mu u_\rho \nabla^\nu u^\rho \rangle$	3	3	2	$4K_5 - 3K_1$
$\langle u_\mu \nabla_\nu u_\rho u^\mu \nabla^\nu u^\rho \rangle$	4	4	3	$4K_3 + K_1$
$\langle u_\mu u^\mu \rangle \langle u_\nu u^\nu \rangle \langle u_\rho u^\rho \rangle$	5			$K_{51}$
$\langle u_\mu u^\mu \rangle \langle u_\nu u_\rho \rangle \langle u^\nu u^\rho \rangle$	6			$K_{56}$
$\langle u_\mu u^\nu \rangle \langle u_\nu u^\rho \rangle \langle u_\rho u^\mu \rangle$	7			$K_{63}$
$\langle u_\mu u^\mu \rangle \langle u_\nu u^\nu u_\rho u^\rho \rangle$	8	5		$K_{50} + 2K_2 + \frac{2}{3}K_6$
$\langle u_\mu u^\mu \rangle \langle u_\nu u_\rho u^\nu u^\rho \rangle$	9	6		$K_{57} - 2K_2 - \frac{2}{3}K_6$
$\langle u_\mu u^\mu u_\nu \rangle \langle u^\nu u_\rho u^\rho \rangle$	10	7		$K_{53}$
$\langle u_\mu u_\nu \rangle \langle u^\mu u^\nu u_\rho u^\rho \rangle$	11			$K_{55} + \frac{2}{3}K_6$
$\langle u_\mu u_\nu \rangle \langle u^\mu u_\rho u^\nu u^\rho \rangle$	12			$K_{62} - \frac{2}{3}K_6$
$\langle u_\mu u_\nu u_\rho \rangle \langle u^\mu u^\nu u^\rho \rangle$	13			$K_{59}$
$\langle u_\mu u_\nu u_\rho \rangle \langle u^\mu u^\rho u^\nu \rangle$	14			$K_{61}$
$\langle u_\mu u^\mu u_\nu u^\nu u_\rho u^\rho \rangle$	15	8	4	$K_{49} + K_1$
$\langle u_\mu u^\mu u_\nu u_\rho u^\nu u^\rho \rangle$	16	9	5	$K_{54} - 2K_1$
$\langle u_\mu u^\mu u_\nu u_\rho u^\rho u^\nu \rangle$	17	10		$K_{52} + \frac{1}{2}K_1$
$\langle u_\mu u_\nu u^\mu u_\rho u^\nu u^\rho \rangle$	18	11		$K_{60} + K_1$
$\langle u_\mu u_\nu u_\rho u^\mu u^\nu u^\rho \rangle$	19	12	6	$K_{58} - \frac{1}{2}K_1$

**Table 2.** The terms of the NNLO NLSM Lagrangian  $\mathcal{L}_6$ . The numbering of the terms is taken from material produced in tandem with [41]; the choice of which terms to keep at small  $N_f$  (see section 2.1) is carried over from [40]. The rightmost column shows how  $K_i$  combine to give  $L_{6,i}$  when the overcomplete Lagrangian is decomposed.

The measurable LECs are given by  $L_i^r(\mu, d)$  as  $d \rightarrow 4$ , with

$$\Gamma_0 = \frac{N_f}{48}, \quad \Gamma_1 = \frac{1}{16}, \quad \Gamma_2 = \frac{1}{8}, \quad \Gamma_3 = \frac{N_f}{24}. \quad (\text{A.8})$$

Likewise, at NNLO the LECs are split as

$$L_{6,i} = \frac{(c\mu)^{2(d-4)}}{F^2} \left[ L_{6,i}^r(\mu, d) - \Gamma_i^{(2)} \Lambda^2 - \left( \Gamma_i^{(1)} + \Gamma_i^{(L)}(\mu, d) \right) \Lambda \right]. \quad (\text{A.9})$$

The  $\Gamma$ 's for the corresponding renormalisation of the  $K_i$  are given in [53]. Using the rightmost column of table 2, the renormalisation of the minimal  $\mathcal{L}_6$  is given in table 3.

## A.2 Explicit divergences

In analogy with (A.7), we define

$$\mathcal{M}_{4,R} = (c\mu)^{d-4} \left[ \mathcal{M}_{4,R}^r(\mu, d) + \mathcal{M}_{4,R}^{(1)} \Lambda \right], \quad (\text{A.10})$$

where  $\mathcal{M}_{4,R}$  is some  $\mathcal{O}(p^4)$  stripped amplitude,  $\mathcal{M}_{4,R}^r(\mu, d)$  is the corresponding measurable amplitude expressed in terms of  $L_i^r(\mu, d)$ , and  $\mathcal{M}_{6,R}^{(1)}$  is its divergence.

$i$	$\Gamma_i^{(2)}$	$16\pi^2\Gamma_i^{(1)}$	$\Gamma_i^{(L)}$
1	$-\frac{5}{72}N_f$	$-\frac{19}{864}N_f$	$-\frac{4}{3}L_3^r - 4L_0^r$
2	$-\frac{5}{9}N_f$	$\frac{1}{864}N_f$	$-\frac{16}{3}L_3^r - \frac{8}{3}L_0^r - \frac{8}{3}N_fL_2^r - 8N_fL_1^r$
3	$-\frac{5}{16} - \frac{5}{96}N_f^2$	$-\frac{1}{96} + \frac{35}{6912}N_f^2$	$-\frac{25}{6}L_2^r - \frac{5}{3}L_1^r - \frac{23}{12}N_fL_3^r - \frac{7}{6}N_fL_0^r$
4	$\frac{5}{16} + \frac{5}{288}N_f^2$	$\frac{1}{96} - \frac{17}{6912}N_f^2$	$\frac{25}{6}L_2^r + \frac{5}{3}L_1^r + \frac{3}{4}N_fL_3^r + \frac{1}{6}N_fL_0^r$
5	$\frac{1}{64}$	$\frac{5}{256}$	$\frac{1}{4}L_2^r$
6	$-\frac{1}{32}$	$\frac{3}{128}$	$-\frac{1}{2}L_2^r$
7	$-\frac{1}{8}$	$-\frac{1}{32}$	$-2L_2^r$
8	$\frac{1}{24}N_f$	$\frac{25}{576}N_f$	$\frac{17}{12}L_3^r + \frac{13}{6}L_0^r + \frac{2}{3}N_fL_2^r - \frac{1}{2}N_fL_1^r$
9	$-\frac{1}{96}N_f$	$-\frac{5}{1152}N_f$	$-\frac{13}{24}L_3^r - \frac{29}{12}L_0^r + \frac{1}{12}N_fL_2^r$
10	$-\frac{1}{64}N_f$	$-\frac{5}{256}N_f$	$-\frac{5}{4}L_3^r + L_0^r$
11	$-\frac{5}{144}N_f$	$-\frac{1}{1728}N_f$	$\frac{2}{3}L_3^r + \frac{4}{3}L_0^r - \frac{2}{3}N_fL_2^r$
12	$-\frac{13}{144}N_f$	$-\frac{53}{1728}N_f$	$-\frac{7}{6}L_3^r - \frac{19}{3}L_0^r - \frac{1}{3}N_fL_2^r$
13	$-\frac{1}{192}N_f$	$\frac{65}{2304}N_f$	$-\frac{3}{4}L_3^r + L_0^r$
14	$\frac{7}{192}N_f$	$-\frac{23}{2304}N_f$	$\frac{5}{4}L_3^r + L_0^r$
15	$\frac{5}{48} + \frac{1}{144}N_f^2$	$-\frac{7}{576} - \frac{25}{6912}N_f^2$	$\frac{5}{6}L_2^r + \frac{5}{3}L_1^r + \frac{1}{6}N_fL_3^r + \frac{1}{3}N_fL_0^r$
16	$-\frac{5}{24} - \frac{1}{96}N_f^2$	$-\frac{19}{576} + \frac{5}{1152}N_f^2$	$-\frac{2}{3}L_2^r - \frac{16}{3}L_1^r - \frac{1}{4}N_fL_3^r - \frac{1}{6}N_fL_0^r$
17	$\frac{5}{96} - \frac{1}{48}N_f^2$	$\frac{43}{576} + \frac{49}{13824}N_f^2$	$\frac{1}{4}L_2^r + \frac{7}{6}L_1^r - \frac{2}{3}N_fL_3^r - \frac{2}{3}N_fL_0^r$
18	$\frac{5}{48} + \frac{1}{64}N_f^2$	$-\frac{67}{576} - \frac{7}{1728}N_f^2$	$\frac{1}{6}L_2^r + 3L_1^r + \frac{17}{24}N_fL_3^r + \frac{1}{12}N_fL_0^r$
19	$-\frac{5}{96} - \frac{1}{144}N_f^2$	$\frac{25}{288} + \frac{5}{4608}N_f^2$	$-\frac{7}{12}L_2^r - \frac{1}{2}L_1^r - \frac{1}{3}N_fL_3^r$

**Table 3.** The coefficients used to renormalise  $\mathcal{L}_6$  as per (A.9).  $L_i^r$  are the renormalised LECs of  $\mathcal{L}_4$  as per (A.7-A.8). Note how the highest power of  $N_f$  in  $\Gamma_i^{(1,2)}$  is 3 minus the number of traces in  $\mathcal{O}_{6,i}$ .

Using this notation and (A.8), the divergence of the  $\mathcal{O}(p^4)$  4-point amplitude (5.4) is

$$-iF^4\mathcal{M}_{4,\{4\}}^{(1)} = N_f \frac{s^2 + t^2 + u^2}{12}, \quad -iF^4\mathcal{M}_{4,\{2,2\}}^{(1)} = \frac{s^2 + t^2 + u^2}{2}. \quad (\text{A.11})$$

These kinematic terms are highly symmetric, more so than the amplitude itself. The divergences of the 6-point amplitude (5.15-5.16) are

$$\begin{aligned}
-iF^6\mathcal{M}_{4,\{6\}}^{(1)} &= \frac{N_f}{12} \left\{ s_{12} \left( s_{12} + s_{34} + \frac{3s_{45}}{2} + s_{234} \right) - \frac{s_{123}s_{234}}{2} \right. \\
&\quad \left. - \frac{(s_{12} + s_{23})(s_{45}^2 + s_{56}^2) + s_{12}s_{23}(s_{45} + s_{56})}{s_{123}} \right\} + [\mathbb{Z}_{\{6\}}] \\
-iF^6\mathcal{M}_{4,\{2,4\}}^{(1)} &= \frac{1}{64} \left\{ 3 \left( t_1^2 + 2t_1t_2 + \frac{t_1t_3}{2} - 3t_1t_5 \right) + 4t_7^2 - 2t_9^2 \right. \\
&\quad + \frac{1}{t_1} \left[ 3(t_2t_3t_4 - 2t_2t_3t_5 - 2t_2t_4t_5 - 2t_3t_4t_5) + 3t_3^2(t_2 + t_4) \right. \\
&\quad \left. \left. + \frac{3(t_3 - 2t_5)}{2} (T_{234}^2 + 2T_{789}^2) \right] \right\} + [\mathbb{Z}_{\{2,4\}}]. \quad (\text{A.12})
\end{aligned}$$

We use the closed basis (D.1), and  $T_{ijk} = t_i + t_j + t_k$ .

An  $\mathcal{O}(p^6)$  analogue of (A.11) can be formed based on (A.9):

$$\mathcal{M}_{6,R} = \frac{(c\mu)^{2(d-4)}}{F^2} \left[ \mathcal{M}_{6,R}^r(\mu, d) - \mathcal{M}_{6,R}^{(2)} \Lambda^2 - \left( \mathcal{M}_{6,R}^{(1)} + \mathcal{M}_{6,R}^{(L)}(\mu, d) \right) \Lambda \right], \quad (\text{A.13})$$

where  $\mathcal{M}_{6,R}^{(2,L)}$  will gain contributions from both (A.7) and (A.9).

Using this notation and the above renormalisation, the divergences of the  $\mathcal{O}(p^6)$  4-point amplitude are (5.6) are

$$\begin{aligned} -iF^4 \mathcal{M}_{6,\{4\}}^{(1)} &= \frac{1}{72} (2t^3 - s^3 - u^3) + \frac{N_f^2}{5184} [8t^3 + 35(s^3 + u^3)], \\ -iF^4 \mathcal{M}_{6,\{4\}}^{(2)} &= \frac{5}{12} (2t^3 - s^3 - u^3) - \frac{5N_f^2}{72} (s^3 + u^3), \\ -iF^4 \mathcal{M}_{6,\{4\}}^{(L)} &= 10 \frac{2L_1^r + 5L_2^r}{9} (2t^3 - s^3 - u^3) \\ &\quad + \frac{2N_f L_0^r}{9} [2t^3 - 7(s^3 + u^3)] - \frac{N_f L_3^r}{9} [2t^3 + 23(s^3 + u^3)], \quad (\text{A.14}) \\ -iF^4 \mathcal{M}_{6,\{2,2\}}^{(1)} &= \frac{N_f}{1296} [s^3 + 58(u^3 + t^3)], \\ -iF^4 \mathcal{M}_{6,\{2,2\}}^{(2)} &= -\frac{5N_f}{108} [8s^3 + 5(u^3 + t^3)], \\ -iF^4 \mathcal{M}_{6,\{2,2\}}^{(L)} &= -16N_f \frac{3L_1^r + L_2^r}{9} (s^3 + t^3 + u^3) \\ &\quad + \frac{2L_0^r}{9} [23(u^3 + t^3) - 8s^3] - \frac{8L_3^r}{9} (u^3 + t^3 + 4s^3), \quad (\text{A.15}) \end{aligned}$$

with the dependence on  $(\mu, d)$  left out for compactness. These expressions do not share the simplicity and symmetry of their  $\mathcal{O}(p^4)$  counterparts. The analogous divergences of the  $\mathcal{O}(p^6)$  6-point amplitude (appendix E.1) are given in [38].

## B The orthogonality of flavour structures

Here, we prove the orthogonality relation (3.32) used in section 3.6 to prove the uniqueness of stripped amplitudes. It relies on notation defined in that and previous sections.

Let  $\sigma, \rho \in \mathcal{S}_n$  be two permutations, and  $Q, R$  be two  $n$ -index flavour splittings. We use these to build two flavour structures, and begin by focusing on the trace in  $\mathcal{F}_\sigma(Q)$  that contains  $a_{\sigma(n)}$  and the trace in  $\mathcal{F}_\rho(R)$  that contains  $a_{\rho(m)}$ , where we have picked  $m$  such that  $\rho(m) = \sigma(n)$ . If there are more traces present, we leave them as passive ‘‘spectators’’ for the time being. Then, we use (3.15) to contract  $a_{\sigma(n)}$  in

$$\mathcal{F}_\sigma(Q) \cdot [\mathcal{F}_\rho(R)]^* = \left[ \langle X a_{\sigma(n-1)} a_{\rho(m-1)} Y \rangle - \frac{1}{N_f} \langle X a_{\sigma(n-1)} \rangle \langle a_{\rho(m-1)} Y \rangle \right] \cdot (\text{spectators}), \quad (\text{B.1})$$

where the product is defined as in (3.32).

From here on, we work only to leading order in  $N_f$ , so we can omit the second term above. (Note that we do not do this because  $N_f$  is necessarily large, but because we wish to use power counting of  $N_f$  to separate orthogonal flavour structures.) We then move on to contracting  $\sigma(n-1)$ , followed by  $\sigma(n-2)$ , and so on. Each time we contract  $\sigma(n-i)$ , the situation may be one of the following cases:

1.  $\rho(m-i) = \sigma(n-i)$ . We carry on through a special case of the contraction identity (3.16), and find

$$\langle X a_{\sigma(n-i)} a_{\sigma(n-i)} Y \rangle = \frac{N_f^2 - 1}{N_f} \langle XY \rangle. \quad (\text{B.2})$$

This may be repeated as long as there are indices left, and we gain a factor of  $N_f$  (plus  $\mathcal{O}(N_f^{-1})$ , which we ignore) each time.

2.  $\rho(m-i) \neq \sigma(n-i)$ , but  $\rho(m') = \sigma(n-i)$  is in the same trace as  $\sigma(n-i)$ . Here, (3.16) (after some reshuffling of  $X$  and  $Y$ ) gives

$$\langle X a_{\sigma(n-i)} Y a_{\sigma(n-i)} \rangle = \left[ \langle X \rangle \langle Y \rangle - \frac{1}{N_f} \langle XY \rangle \right]. \quad (\text{B.3})$$

the second term is suppressed by a factor of  $N_f^{-1}$ , and the first must eventually take a detour through (B.1) before continuing; in any case, this case falls behind case 1 by at least two factors of  $N_f$ .

3.  $\rho(m') = \sigma(n-i)$  is in a different trace than  $\sigma(n-i)$ . This forces us to bring in the spectator trace containing  $\rho(m')$  and go back to (B.1), so this case falls behind case 1 by at least one factor of  $N_f$ .
4. The trace is empty. We gain a factor of  $\langle \mathbb{1} \rangle = N_f$ , and if there are no spectator traces left, we are done. Otherwise, we bring in the next pair of spectators and continue from (B.1).

If  $Q = R = \{n\}$  and  $\sigma \equiv \rho \pmod{\mathbb{Z}_R}$ , we will only encounter case 1 until we finish with a case 4, and will gain a total factor of  $N_f^n [1 + \mathcal{O}(N_f^{-2})]$ . If  $Q = R \neq \{n\}$  on the other hand, we will encounter case 4 at each split, but the leading power of  $N_f$  stays the same.

If  $\sigma \not\equiv \rho \pmod{\mathbb{Z}_R}$ , we must eventually encounter case 2, so this falls behind the  $\sigma \equiv \rho \pmod{\mathbb{Z}_R}$  case by at least two powers of  $N_f$ . If  $Q \neq R$ , we will encounter case 3 (without a corresponding case 4) whenever there is a mismatch in the flavour splits, so we will fall behind the  $Q = R$  case by at least one power of  $N_f$ . This is the reason for the values of  $\gamma$  stated below (3.32).

Thus, we have proven

$$\mathcal{F}_\sigma(Q) \cdot [\mathcal{F}_\rho(R)]^* = N_f^n \begin{cases} 1 + \mathcal{O}(N_f^{-2}) & \text{if } Q = R \text{ and } \sigma \equiv \rho \pmod{\mathbb{Z}_R}, \\ \mathcal{O}(N_f^{-\gamma}) & \text{otherwise } (\gamma \geq 1) \end{cases} \quad (\text{B.4})$$

which is (3.32).

## C The double soft limit

This appendix provides a derivation of (4.4), which is used to calculate the double soft limit of stripped amplitudes. We start by quoting (4.2), which is proven in [36] and gives the double soft limit of the full amplitude:

$$\lim_{\varepsilon \rightarrow 0} \mathcal{M}_{m,n+2}^{aba_1 \cdots a_n}(\varepsilon p, \varepsilon q, p_1, \dots, p_n) = -\frac{1}{F^2} \sum_{i=1}^n f^{abc} f^{a_i dc} \frac{p_i \cdot (p-q)}{p_i \cdot (p+q)} \mathcal{M}_{m,n}^{a_1 \cdots a_{(i-1)} da_{(i+1)} \cdots a_n}(p_1, \dots, p_n). \quad (\text{C.1})$$

In order to find the corresponding expression for a stripped amplitude, we project it out by contracting both sides with  $[\mathcal{F}_{\text{id}}(R)]^*$  over all flavour indices (see (3.12) and section 3.6). On the left-hand side of (C.1), this will project out  $\lim_{\varepsilon \rightarrow 0} \mathcal{M}_{m,R}(\varepsilon p, \varepsilon q, p_1, \dots)$ . For simplicity, we start with  $R = \{n+2\}$  before moving on to the general multi-trace case. According to (3.12), the right-hand side of (C.1) has the form (schematically, with kinematic terms omitted)

$$\sum_{\sigma \in \mathcal{S}_n / \mathbb{Z}_n} f^{abc} f^{a_i dc} \langle a_{\sigma(1)} \cdots a_{\sigma(i-1)} da_{\sigma(i+1)} \cdots a_{\sigma(n)} \rangle \quad (\text{C.2})$$

plus flavour-split structures, but those can be ignored due to (3.32). We have omitted the algebra generators for readability;  $a_i$  means  $t^{a_i}$ . The structure constants can be contracted in using (3.15) and  $f^{abc} = -i \langle t^a [t^b, t^c] \rangle$ , leaving

$$- \langle a_{\sigma(1)} \cdots a_{\sigma(i-1)} [[a, b], a_{\sigma(i)}] a_{\sigma(i+1)} \cdots a_{\sigma(n)} \rangle. \quad (\text{C.3})$$

With appendix B in mind, we immediately see that this is orthogonal to  $\mathcal{F}_{\text{id}}(n+2)$  unless  $\sigma = \text{id}$ . The nested commutators expand to

$$[[a, b], a_i] = aba_i - baa_i - a_i ab + a_i ba. \quad (\text{C.4})$$

Since  $a$  comes before  $b$  in  $\mathcal{F}_{\text{id}}(n+2)$ , the second and fourth terms vanish under the projection. Also,  $ab$  occurs at the beginning (or, equivalently, the end) of the flavour structure, so the first term only contributes when  $i = 1$ , and the third term only contributes when  $i = n$ . This collapses the sum in (C.1) to those two cases, leaving

$$\lim_{\varepsilon \rightarrow 0} \mathcal{M}_{m,\{n+2\}}(\varepsilon p, \varepsilon q, p_1, \dots, p_n) = \frac{1}{F^2} \left\{ \frac{p_1 \cdot (p-q)}{p_1 \cdot (p+q)} - \frac{p_n \cdot (p-q)}{p_n \cdot (p+q)} \right\} \mathcal{M}_{m,\{n\}}(p_1, \dots, p_n). \quad (\text{C.5})$$

If we now move on to general  $R$ , we see that  $a$  and  $b$  must reside in the same trace, since the nested commutator on the right-hand side is inside a single trace. This is essentially the condition stated for the validity of (4.4), with  $(p_n, p, q, p_1)$  mapping to  $(p_{i-1}, p_i, p_j, p_{j+1})$ . The trace they reside in can be treated exactly like the single-trace flavour structure of (C.5), and all other traces in the flavour structure follow along as ‘‘spectators’’, as in a

normal application of (3.32). The reduction  $\{n+2\} \rightarrow \{n\}$  in (C.5) then generalises to  $R \rightarrow R'$  as described below (4.4). This generalisation therefore results in (4.4), which is thereby proven.

## D Closed Mandelstam bases

Here, we show the derivation of closed Mandelstam bases for all 6-particle flavour structures as described in section 4.2. Note that neither basis is unique, and that better basis choices may exist.

### D.1 The basis for $R = \{2, 4\}$

This is the only basis other than  $\mathcal{B}_{\{6\}}$  that is needed at  $\mathcal{O}(p^4)$ . This flavour split permits four different propagator momenta (corresponding to the labellings in (3.21)). Since  $\mathbb{Z}_{\{2,4\}}$  is Abelian and rather small, it is simple to handle, and some inspired trial-and-error gives the closed basis  $\mathcal{B}_{\{2,4\}} = \{t_1, \dots, t_9\}$  with elements<sup>11</sup>

$$\begin{aligned} t_1 &= s_{123}, & t_2 &= s_{124}, & t_3 &= s_{125}, & t_4 &= s_{126}, \\ t_5 &= s_{45} + s_{56} + \frac{s_{125} - s_{123}}{2}, & t_6 &= s_{45} - s_{56} + \frac{2s_{124} - (s_{124} + s_{125})}{2}, \\ t_7 &= s_{14} + s_{15} + \frac{s_{123} + s_{126}}{2}, & t_8 &= s_{15} + s_{16} + \frac{s_{123} + s_{124}}{2}, \\ t_9 &= s_{14} + s_{16} + \frac{s_{123} + s_{125}}{2}. \end{aligned} \tag{D.1}$$

Under the action of  $\mathbb{Z}_{\{2,4\}}$ , they transform as

$$\begin{aligned} 21\ 3456 : & \quad \{t_1, \dots, t_6, t_7, t_8, t_9\} \rightarrow \{t_1, \dots, t_6, -t_7, -t_8, -t_9\}, \\ 12\ 4563 : & \quad \{t_1, \dots, t_6, t_7, t_8, t_9\} \rightarrow \{t_2, t_3, t_4, t_1, t_5, -t_6, +t_8, -t_7, -t_9\}, \end{aligned} \tag{D.2}$$

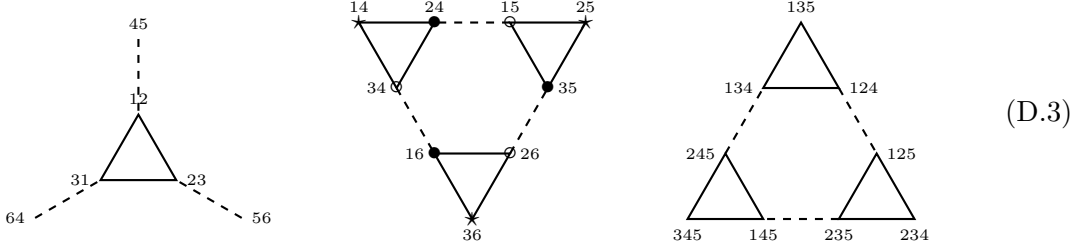
where the first permutation cycles the 2-trace, and the second cycles the 4-trace; together, they generate all of  $\mathbb{Z}_{\{2,4\}}$ . Note that  $\mathbb{Z}_{\{2,4\}}$  does not act as a true permutation on the basis, since some elements change sign. This appears to be unavoidable, but is not a problem — in fact, any complex phase can be applied without hindering simplification.

### D.2 The basis for $R = \{3, 3\}$

The group  $\mathbb{Z}_{\{3,3\}}$  is generated by the permutations  $g_1 = 231\ 456$  and  $g_2 = 456\ 123$ . The group is not abelian, which makes its effects less predictable. Among all kinematic invariants, only  $s_{123}$  maps to itself under both generators, and is also the only squared propagator momentum permitted by this flavour structure. The other 24 invariants decompose into a sextuplet and two nonets under the group, and can be mapped out in a variant of a Cayley

<sup>11</sup>This basis is a slight improvement over the one used in [37]. It modifies  $t_5$  and  $t_6$  so that they map to themselves under  $\mathbb{Z}_{\{2,4\}}$ .

graph:



Each node in the graph represents  $s_{ij\dots}$  and is marked with  $ij\dots$ . The action of  $g_1$  is represented by following the solid-drawn triangles clockwise, and  $g_2$  is represented by following the dashed lines.

We must now extract 9 basis elements  $t_1, \dots, t_9$  that are closed under  $\mathbb{Z}_{\{3,3\}}$ . In the first nonet, we have marked three sets of invariants with  $\star$ ,  $\bullet$  and  $\circ$ . They map to each other as  $(\star, \bullet, \circ) \rightarrow (\bullet, \circ, \star)$  under  $g_1$  and as  $(\star, \bullet, \circ) \rightarrow (\star, \circ, \bullet)$  under  $g_2$ , so suitable linear combinations of the elements in each set will be closed under  $\mathbb{Z}_{\{3,3\}}$ . Similar constructions taken from the sextet and the other nonet turn out not to be linearly independent from these.

Unfortunately, it appears impossible to form a basis that contains the propagator momentum  $s_{123}$  as an element, but since there is only one propagator, this is not as much of a problem as it would be under a group that supports more operators. Also, it appears impossible to form real linear combinations without sacrificing either linear independence or closedness. Guided by the fact that  $g_1$  has period 3, we instead insert the third root of unity,  $\omega = e^{2\pi i/3}$ , and find the closed and complete basis  $\mathcal{B}_{\{3,3\}}$  with elements<sup>12</sup>

$$\begin{aligned}
t_1 &= -\frac{s_{36} + s_{14} + s_{25}}{3}, & t_2 &= -\frac{s_{24} + s_{35} + s_{16}}{3}, & t_3 &= -\frac{s_{15} + s_{26} + s_{34}}{3}, \\
t_6 &= \frac{s_{36} + \omega s_{14} + \omega^2 s_{25}}{3}, & t_4 &= \frac{s_{24} + \omega s_{35} + \omega^2 s_{16}}{3}, & t_5 &= \frac{s_{15} + \omega s_{26} + \omega^2 s_{34}}{3}, \\
t_9 &= \frac{\omega^2 s_{36} + \omega s_{14} + s_{25}}{3}, & t_7 &= \frac{\omega^2 s_{24} + \omega s_{35} + s_{16}}{3}, & t_8 &= \frac{\omega^2 s_{15} + \omega s_{26} + s_{34}}{3},
\end{aligned} \tag{D.4}$$

In each row above, the first basis element comes from the  $\star$  set, the second from the  $\bullet$  set, and the third from the  $\circ$  set. The propagator momentum is  $s_{123} = \frac{3}{2}(t_1 + t_2 + t_3)$ . The basis transforms as

$$\begin{aligned}
g_1 : & \quad \{t_1, t_2, t_3, t_4, t_5, t_6, t_7, t_8, t_9\} \rightarrow \{t_2, t_3, t_1, \omega t_5, \omega t_6, \omega t_4, \omega^2 t_8, \omega^2 t_9, \omega^2 t_7\}, \\
g_2 : & \quad \{t_1, t_2, t_3, t_4, t_5, t_6, t_7, t_8, t_9\} \rightarrow \{t_1, t_3, t_2, t_4, t_6, t_5, t_7, t_9, t_8\}.
\end{aligned} \tag{D.5}$$

Since stripped amplitudes are real, the complex basis must be compensated for by complex coefficients. Still,  $\mathcal{B}_{\{3,3\}}$  is just as valid as a real basis, and is useable for simplification.

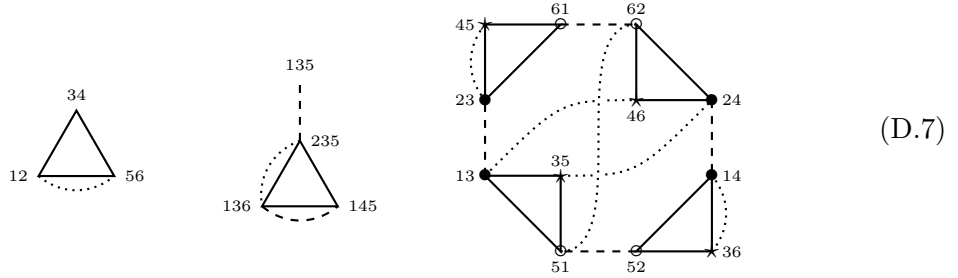
<sup>12</sup>The basis presented in [37] was not complete. This mistake was not discovered until after its publication, and is corrected here at the cost of losing the propagator.

### D.3 The basis for $R = \{2, 2, 2\}$

The group  $\mathbb{Z}_{\{2,2,2\}}$  is also non-abelian, and can be tackled similarly to  $\mathbb{Z}_{\{3,3\}}$ . We choose the generators  $g_1 = 34\ 56\ 12$ ,  $g_2 = 21\ 34\ 56$  and  $g_3 = 65\ 43\ 21$  with the hopes that they be well-behaved, since  $\mathcal{B}_{\{6\}}$  is closed under two of them. This flavour structure permits six propagators that form a sextet under the group. The Cayley graph is



where  $g_1$  and  $g_2$  are represented as in (D.3), and the dotted lines represent the action of  $g_3$ . The remaining invariants decompose into a triplet, a quadruplet, and a 12-plet:



Like in (D.3), we have marked three closed sets of  $s_{ij}$ 's. From these, it is possible to construct three linearly independent elements that close the basis without need for the less structured triplet and quadruplet. Thus,  $\mathcal{B}_{\{2,2,2\}}$  has elements

$$\begin{aligned}
 t_1 &= s_{123}, & t_2 &= s_{126}, & t_3 &= s_{156}, & t_4 &= s_{124}, & t_5 &= s_{125}, & t_6 &= s_{134}, \\
 t_7 &= \frac{s_{61} - s_{62} + s_{52} - s_{51}}{2}, & t_8 &= \frac{s_{23} - s_{24} + s_{14} - s_{13}}{2}, & t_9 &= \frac{s_{45} - s_{46} + s_{36} - s_{35}}{2},
 \end{aligned}
 \tag{D.8}$$

where the factors of  $1/2$  remove some large powers of 2 that show up when writing amplitudes in this basis. Unlike in  $\mathcal{B}_{\{3,3\}}$ , there was no need to resort to complex numbers. The basis transforms as

$$\begin{aligned}
 g_1 &: \{t_1, t_2, t_3, t_4, t_5, t_6, t_7, t_8, t_9\} \rightarrow \{t_1, t_2, t_6, t_4, t_5, t_3, -t_7, -t_8, t_9\}, \\
 g_2 &: \{t_1, t_2, t_3, t_4, t_5, t_6, t_7, t_8, t_9\} \rightarrow \{t_2, t_3, t_1, t_5, t_6, t_4, t_8, t_9, t_7\}, \\
 g_3 &: \{t_1, t_2, t_3, t_4, t_5, t_6, t_7, t_8, t_9\} \rightarrow \{t_1, t_3, t_2, t_4, t_6, t_5, t_7, t_9, t_8\}.
 \end{aligned}
 \tag{D.9}$$

No element is a fixed point, which makes the basis harder to work in.

## E Explicit amplitudes

### E.1 The $\mathcal{O}(p^6)$ 6-point amplitude

This amplitude has been simplified using the closed bases of appendix D. The terms were reduced to coset representatives in FODGE followed by manual post-processing. Greater

simplification might be possible for some terms. The amplitude consists of four stripped amplitudes with flavour split  $\{6\}$ ,  $\{2, 4\}$ ,  $\{3, 3\}$ , and  $\{2, 2, 2\}$ .

There are three diagrams with a single-trace flavour structure:

$$(E.1)$$

The corresponding stripped amplitude is

$$\begin{aligned}
& -iF^8 \mathcal{M}_{6,\{6\}} \\
& = 2(L_3 + 2L_0)^2 \{2(s_{12} + s_{23})^2(s_{45} + s_{56}) - s_{123}(s_{12} + s_{23})(s_{45} + s_{56})\} \\
& + 16L_3L_0s_{12}s_{23}(s_{45} + s_{56}) \\
& - 8(L_0^2 + L_3L_0) \frac{(s_{12} + s_{23})^2(s_{45} + s_{56})^2}{s_{123}} - 2L_3^2 \frac{(s_{12}^2 + s_{23}^2)(s_{45}^2 + s_{56}^2)}{s_{123}} \\
& + L_{6,3} \left\{ \left[ s_{123}s_{34} - \frac{s_{123}s_{234}}{2} \right] (s_{12} + [\mathbb{Z}_6]) - s_{12}s_{23}s_{34} \right. \\
& \quad \left. + \frac{2(s_{12} + s_{45})^3 + (s_{12}^3 + s_{45}^3)}{3} - \frac{[(s_{12} + s_{23})^3 + 2(s_{12}^3 + s_{23}^3)](s_{45} + s_{56})}{3s_{123}} \right\} \\
& + L_{6,4} \left\{ s_{123}s_{234}s_{345} + \frac{s_{123}^2}{2}(s_{234} + s_{345} - 2s_{34}) \right. \\
& \quad - 2s_{123}s_{234}(2s_{12} + s_{23} + 2s_{34}) - \frac{s_{12}s_{45}}{2}(s_{123} + s_{345}) \\
& \quad + s_{123} [s_{12} + s_{56} + 2s_{12}s_{34} + 2s_{34}s_{56} + 4s_{34}(s_{23} + s_{34} + s_{45})] \\
& \quad \left. + \frac{(s_{12} + s_{45})^3}{2} - \frac{(s_{12} + s_{23})^3(s_{45} + s_{56})}{s_{123}} \right\} \\
& - L_{6,15} \{s_{12}s_{45}s_{56}\} \\
& + L_{6,16} \left\{ s_{12}(s_{34} + s_{45})(s_{123} + s_{345}) - s_{12}s_{123}s_{345} - s_{12}s_{34}s_{56} - \frac{s_{12}s_{45}}{2}(s_{12} + [\mathbb{Z}_6]) \right\} \\
& + L_{6,17} \{s_{12}s_{45}(s_{123} + s_{345} - s_{12} - s_{45})\} \\
& + L_{6,18} \left\{ (s_{12} + s_{45} + s_{234}^2)(s_{123} + s_{345}) - s_{12}s_{234}(s_{123} + [\mathbb{Z}_6]) - 4s_{12}s_{123}s_{345} \right. \\
& \quad \left. + 2s_{12}s_{234}(s_{23} + s_{34} + s_{45} + s_{56} + s_{61}) - 2s_{12}s_{34}(s_{23} + s_{45} + s_{56} + s_{61}) \right\} \\
& + L_{6,19} \left\{ 2s_{123}s_{234}s_{345} + 3s_{234}^2(s_{123} + s_{345}) - 3s_{12}s_{234}(s_{123} + [\mathbb{Z}_6]) - 6s_{12}s_{123}s_{345} \right. \\
& \quad \left. + 6s_{12}s_{234}(s_{23} + s_{34} + s_{56} + s_{61}) - 6s_{12}s_{23}s_{34} - 2s_{12}s_{34}s_{56} \right\} \\
& + [\mathbb{Z}_6].
\end{aligned} \tag{E.2}$$

The “+  $[\mathbb{Z}_6]$ ” acts on all terms in the amplitude.

There are also three diagrams with a  $\{2, 4\}$ -split flavour structure:

$$(E.3)$$

Using the closed basis (D.1), the stripped amplitude is

$$\begin{aligned}
& -iF^8 \mathcal{M}_{6,\{2,4\}} \\
&= L_0 L_1 \left\{ t_1 \left[ -t_1^2 + t_2^2 + 2t_3(3t_2 + t_3 - 2t_5) + t_4^2 + 4t_5^2 \right] - \frac{T_{234}^2(t_3 - 2t_5)^2}{t_1} \right\} \\
&+ L_0 L_2 \left\{ t_1 \left[ t_1 \left( 2t_5 - \frac{5t_1}{4} \right) + t_2 \left( \frac{t_2}{4} + \frac{3t_2}{2} + 4t_5 \right) \right. \right. \\
&\quad \left. \left. + 3t_3 \left( \frac{t_3}{2} - t_5 \right) + \frac{t_4^2}{4} - 3t_5^2 + T_{789}^2 \right] - \frac{(t_3 - 2t_5)^2(T_{234}^2 + 4T_{789}^2)}{4t_1} \right\} \\
&+ L_3 L_1 \left\{ -\frac{t_1^3}{2} + 2t_1^2(t_5 - t_6) \right. \\
&\quad + t_1 \left[ 2t_2(t_3 + 2t_5 + t_6) + t_3(5t_3 + t_5 - 3t_6) - \frac{3t_4^2}{2} + t_5^2 + t_6^2 \right] \\
&\quad + \frac{1}{t_1} \left[ -t_2^3(t_2 + t_3 + 2t_4 + 2t_6) + t_2^2 \left( \frac{t_3^2}{2} + t_3(t_5 - 3t_6) - t_4^2 - 4t_4t_6 \right) \right. \\
&\quad \quad + t_2(t_3^2t_4 + t_3t_4^2) + 2t_2t_3t_4(t_5 - t_6) - 2t_2t_4^2t_6 - \frac{t_4^4}{2} \\
&\quad \quad \left. \left. + t_3^3(-t_4 + t_5 + t_6) - \frac{t_3^2t_4^2}{2} + (t_5 + t_6)(t_3t_4^2 + 2t_3^2t_4) - T_{234}^2(t_5^2 + t_6^2) \right] \right\} \\
&+ L_3 L_2 \left\{ -\frac{9t_1^3}{8} + t_1^2 \frac{t_5 + t_6}{2} \right. \\
&\quad + t_1 \left[ t_2 \left( \frac{11t_2}{2} + \frac{t_3}{2} + 3t_5 + \frac{5t_6}{2} \right) + \frac{t_3}{4} (5t_3 + t_5 + t_6) - \frac{3(t_5^2 + t_6^2)}{4} \right. \\
&\quad \quad \left. - \frac{7t_4^2}{8} + t_7(t_9 - 3t_8) + 5t_8t_9 + \frac{t_8^2 + t_9}{2} \right] + t_5(2t_7^2 + t_9^2) + 2t_6t_7t_8 \\
&\quad + \frac{1}{t_1} \left[ \frac{T_{789}^2}{4} \left( [2t_2 - t_3]^2 + [2t_5 + 2t_6 - t_3]^2 + 8t_6[t_2 - t_5] \right) \right. \\
&\quad \quad - \frac{T_{234}^2}{4}(t_5^2 + t_6^2) + \frac{t_5 + t_6}{4}(2t_3^2t_4 + t_3t_4^2) - \frac{t_4^4}{4} - \frac{t_3^3}{4}(t_3 + 2t_4 + 2t_6) \\
&\quad \quad + \frac{t_2^2}{8}(t_3^2 + 2t_3t_5 - 6t_3t_6 - 2t_4^2 - 8t_4t_6) \\
&\quad \quad \left. \left. + \frac{t_2}{2} \left( \frac{t_3^2}{2}[t_4 + 2t_5] + \frac{t_3}{2}[t_4^2 + 2t_4t_5 - 2t_4t_6] - t_4^2t_6 \right) \right] \right\} \\
&+ L_{6,1} \mathcal{H}(3) + L_{6,2} \mathcal{H}(-1) \\
&+ L_{6,8} \left\{ \frac{t_1}{4} [t_2^2 - 2t_3^2 + t_4^2 - 2(t_5^2 + 2t_6^2) + 2t_6(t_1 + t_3)] \right\} \\
&+ L_{6,9} \left\{ -t_1 \left[ 4t_5^2 + \frac{t_2^2 + t_4^2}{2} + t_2t_3 - t_5(t_1 + 2t_2 + t_3) \right] \right\} \\
&+ L_{6,11} \left\{ \frac{t_1^3}{16} - \frac{t_1}{16} [t_2^2 - t_3^2 + t_4^2 + 4(t_8^2 - t_7^2) + 2t_2(t_5 + t_6) + 4t_9(t_8 + t_7)] \right. \\
&\quad \left. - \frac{t_5t_9^2}{8} - \frac{t_6t_7^2}{4} \right\}
\end{aligned}$$

$$\begin{aligned}
& + L_{6,12} \left\{ \frac{t_1^3}{16} - \frac{t_1}{16} [(t_2 + t_3)^2 + t_4^2 + 4(t_7 + t_8)^2 + 4t_9^2 - 4t_3t_5] + t_5 \frac{2t_7^2 - t_9^2}{4} \right\} \\
& + [\mathbb{Z}_{\{2,4\}}], \tag{E.4}
\end{aligned}$$

where  $T_{ijk} = t_i + t_j + t_k$ , and

$$\begin{aligned}
\mathcal{H}(\eta) &= \frac{3t_1^3}{128} - \frac{3t_1^2t_5}{32} \\
& + t_1 \left[ \frac{9t_2^2}{128} + t_2 \frac{3t_3 - 5t_5}{32} + \frac{t_3^2}{32} - \frac{5t_3t_5}{64} + \frac{9t_4^2}{128} + \frac{\eta}{32} (t_7 + t_8 - t_9)^2 + \frac{\eta}{8} (t_7^2 + t_8^2 - t_9^2) \right] \\
& - \eta t_5 \frac{2t_7^2 + t_9^2}{16} + \frac{3}{16t_1} \left[ t_2^3 \frac{t_3 - 2t_5}{24} + \frac{t_2^2t_3}{8} (t_3 + t_4 - 2t_5) - \frac{t_2^2t_4t_5}{4} \right. \\
& \quad + \frac{t_2t_3^2}{8} (t_3 + 2t_4 - 2t_5) + \frac{t_2t_3}{8} (t_4^2 - 4t_4t_5) + \frac{t_2t_4^2t_5}{4} \\
& \quad + \frac{t_3^3}{24} (t_3 + 3t_4 + 2t_5) + \frac{t_3^2t_4}{8} (t_4 - 2t_5) + \frac{t_4^4}{24} - \frac{t_4^2t_5}{12} (3t_3 + t_4) \\
& \quad \left. + \frac{\eta T_{789}^2}{6} (t_3^2 + t_2t_3 - t_2t_5 + t_3t_4 - 2t_3t_5 - 2t_4t_5) \right] \tag{E.5}
\end{aligned}$$

is used for compactness.

There are two diagrams with a  $\{3, 3\}$  flavour split:

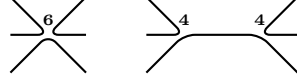
$$\begin{array}{ccc}
\begin{array}{c} \diagup \quad \diagdown \\ \diagdown \quad \diagup \\ \diagup \quad \diagdown \\ \diagdown \quad \diagup \end{array} & \begin{array}{c} \diagup \quad \diagdown \\ \diagdown \quad \diagup \\ \text{---} \\ \diagup \quad \diagdown \\ \diagdown \quad \diagup \end{array}
\end{array} \tag{E.6}$$

Using the closed basis (D.4), the stripped amplitude is

$$\begin{aligned}
& -iF^8 \mathcal{M}_{6,\{3,3\}} \\
& = 64(L_0 + L_3)^2 \left\{ (s_{12} + s_{23}) (s_{45}^2 + s_{45}s_{56} + s_{56}^2) + (s_{12}^2 + s_{12}s_{23} + s_{23}^2) (s_{45} + s_{56}) \right. \\
& \quad \left. - \frac{(s_{12}^2 + s_{12}s_{23} + s_{23}^2) (s_{45}^2 + s_{45}s_{56} + s_{56}^2)}{s_{123}} \right\} \\
& + L_{6,10} \left\{ \frac{t_1^3}{4} - (t_4^4 + t_7^3) + \frac{t_1t_2t_3}{2} + t_4t_5t_6 + t_7t_8t_9 + \frac{3t_1t_2^2}{2} + 6\omega t_1t_5(t_9 - t_8) \right\} \\
& + L_{6,13} \{t_1^3 - (t_4^3 + t_7^3) - 3\omega t_1t_4t_7\} \\
& + L_{6,14} \{t_1t_2t_3 - (t_4t_5t_6 + t_7t_8t_9) + 6\omega t_1t_5t_9\} \\
& + [\mathbb{Z}_{\{3,3\}}], \tag{E.7}
\end{aligned}$$

where  $\omega = e^{2\pi i/3}$  is a third root of unity. The contribution from the singlet diagram turns out to be simpler to express in the standard basis  $\mathcal{B}_{\{6\}}$  than in the closed basis.

Lastly, there are two diagrams for the  $\{2, 2, 2\}$  flavour split:


(E.8)

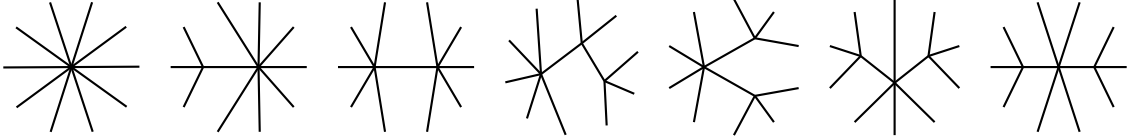
Using the closed basis (D.8), the stripped amplitude is

$$\begin{aligned}
& -iF^8 \mathcal{M}_{6,\{2,2,2\}} \\
&= L_1^2 \left\{ -\frac{t_1^3}{2} + t_1(2t_2^2 + 6t_2t_4 + t_4^2) \right. \\
&\quad \left. - \frac{1}{t_1} \left[ \frac{t_4^4}{2} + (t_2 + t_5)^2(t_4^2 + 4t_3t_4t_3^2) + 2t_2t_3t_5t_6 + 2t_2t_3^2t_5 + 8t_4^2t_2t_3 + 4t_4^3t_2 \right] \right\} \\
&+ L_1L_2 \left\{ t_1t_8^2 + \frac{3t_1t_4^2}{2} + \frac{t_1t_2}{2}(4t_9 + 5t_4 - 8t_3 - 5t_2) - \frac{5t_1^3}{4} \right. \\
&\quad - \frac{1}{t_1} \left[ \frac{t_2^2}{2} (t_2^2 + 2t_3^3 + 3t_4^2 - t_5^2 + 4t_9^2 + 2t_2t_4 + 4t_2t_9 + 8t_4t_9 + 8t_3t_4 + 4t_3t_6) \right. \\
&\quad \quad + t_2t_3(4t_4^2 + 4t_4t_5 + t_5t_6) + 2t_2t_9(t_4^2 - t_5^2) + 2t_2t_9^2(t_4 + t_5) \\
&\quad \quad \left. + 2t_2t_4^3 + \frac{t_2t_4^2t_5}{2} - t_2t_4t_5^2 + t_4^2t_8^2 + \frac{t_4^4}{4} \right] \left. \right\} \\
&- L_2^2 \left\{ \frac{21t_1^3}{32} + \frac{3t_1t_8^2}{4} - \frac{11t_1t_4^2}{16} + \frac{t_1t_2}{4}(t_4 + 6t_3 + t_2 - 10t_9) \right. \\
&\quad + \frac{1}{4t_1} \left[ \frac{t_2^2}{2} (t_2^2 + 2[t_3 + t_4]^2 - t_5^2 + 4[t_8^2 + t_9^2] + 2t_2[t_4 + 2t_9] + 8t_4t_9 + 8t_3t_8) \right. \\
&\quad \quad + t_2t_3 (2t_4^2 + 2t_4t_5 + t_5t_6 - 4t_5t_8 + 8t_8t_9) \\
&\quad \quad + t_2t_4 (t_4^2 + 2t_4t_9 - t_5^2 + 4t_9^2) - 2t_2t_5^2t_9 + 2t_2t_5 (t_9^2 - t_8^2) \\
&\quad \quad \left. + t_8^2 (t_4^2 + 2t_9^2 + 8t_2t_9) + \frac{t_4^4}{8} \right] \left. \right\} \\
&+ [\mathbb{Z}_{\{2,2,2\}}] \tag{E.9}
\end{aligned}$$

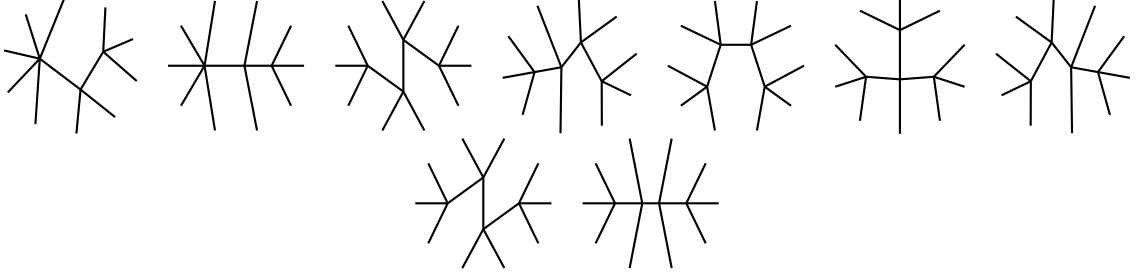
This completes the amplitude.

## E.2 The $\mathcal{O}(p^2)$ 10-point amplitude

Due to the absence of flavour splits,  $\mathcal{O}(p^2)$  amplitudes are relatively easy to extend to many legs. The 10-point amplitude, which is also computed in [36], is given by the 16 diagrams<sup>13</sup>



<sup>13</sup>The circular shape is a result of the automatic diagram drawing in FODGE. The external legs are evenly distributed around a circle, and the location of each vertex is generated from the mean locations of all legs and vertices connected to it.



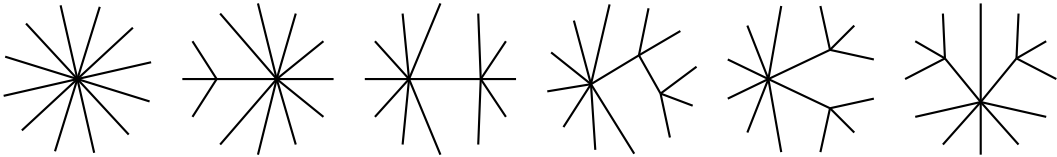
and has the stripped amplitude

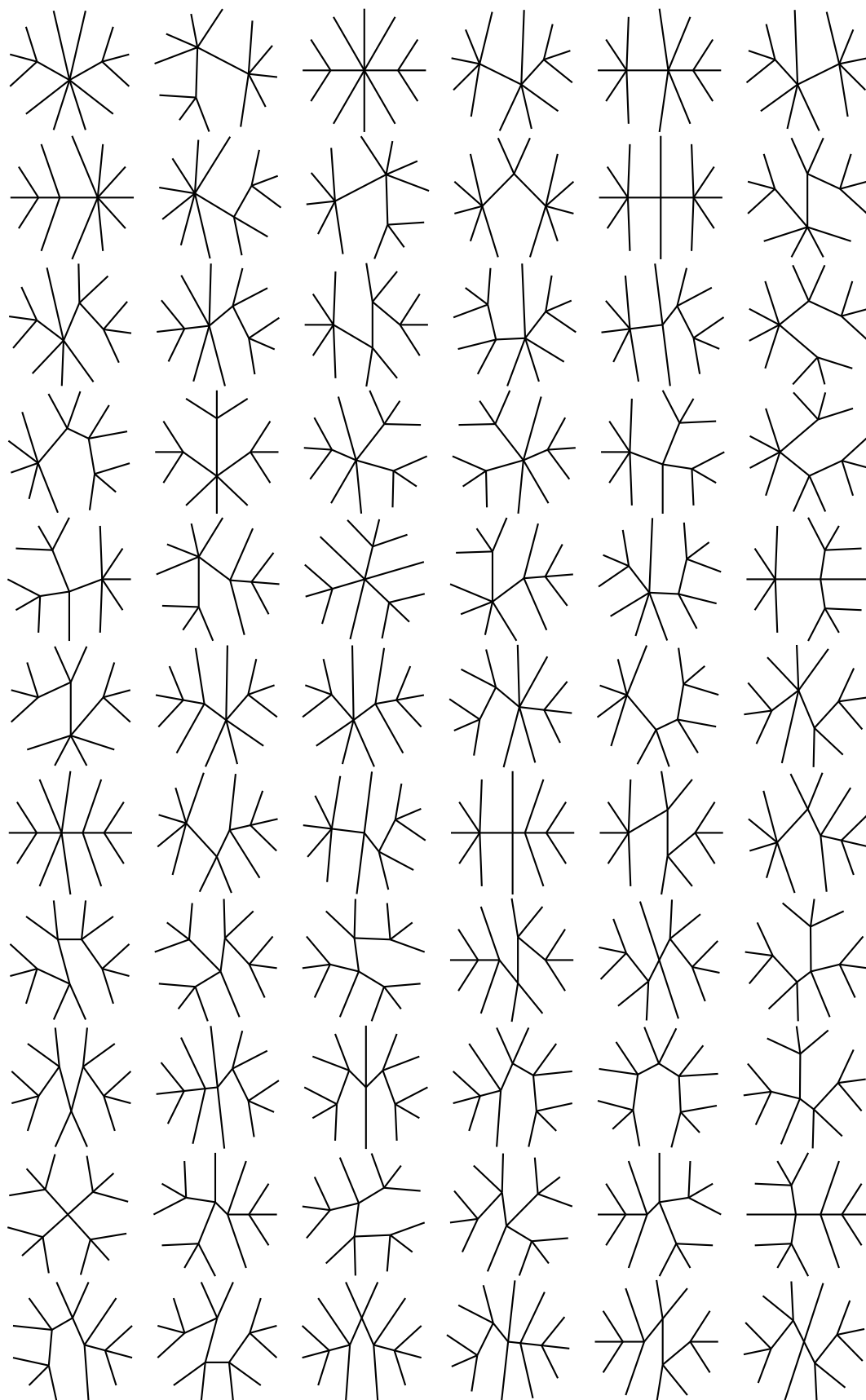
$$\begin{aligned}
-16iF^8 \mathcal{M}_{2,\{10\}} &= 5s_{12} + 2s_{1234} \\
&- \frac{(s_{12} + s_{23} + s_{34} + s_{45} + s_{\overline{14}} + s_{\overline{25}})(s_{67} + s_{78} + s_{89} + s_{9A} + s_{\overline{69}}s_{\overline{7A}})}{2s_{\overline{15}}} \\
&- \frac{s_{12} + s_{23}}{s_{123}} \left\{ 2(s_{45} + s_{56} + s_{67} + s_{78} + s_{89} + s_{9A}) + 2(s_{\overline{A3}} + s_{\overline{14}}) \right. \\
&- \frac{(s_{67} + s_{78})(s_{45} + s_{9A} + s_{\overline{A3}} + s_{\overline{14}} + s_{\overline{58}} + s_{\overline{69}})}{2s_{678}} \\
&- \frac{(s_{78} + s_{89})(s_{45} + s_{56} + s_{\overline{14}} + s_{\overline{47}} + s_{\overline{7A}} + s_{\overline{69}})}{s_{789}} \\
&- \left. \frac{(s_{89} + s_{9A})(s_{45} + s_{56} + s_{67} + s_{\overline{14}} + s_{\overline{47}} + s_{\overline{7A}})}{s_{89A}} \right. \\
&+ \frac{s_{9A} + s_{\overline{A3}}}{s_{48}} \left[ \frac{(s_{67} + s_{78})(s_{45} + s_{\overline{58}})}{2s_{678}} - (s_{45} + s_{56} + s_{67} + s_{78} + s_{\overline{47}} + s_{\overline{58}}) \right] \\
&+ \frac{s_{\overline{A3}} + s_{\overline{14}}}{s_{59}} \left[ \frac{(s_{67} + s_{78})(s_{\overline{58}} + s_{\overline{69}})}{2s_{678}} - (s_{56} + s_{67} + s_{78} + s_{89} + s_{\overline{58}} + s_{\overline{69}}) \right] \\
&+ \frac{s_{\overline{14}} + s_{45}}{s_{15}} \left[ - (s_{67} + s_{78} + s_{89} + s_{9A} + s_{\overline{69}} + s_{\overline{7A}}) \right. \\
&\quad \left. + \frac{(s_{67} + s_{78})(s_{\overline{69}} + s_{9A})}{2s_{678}} + \frac{(s_{78} + s_{89})(s_{\overline{69}} + s_{\overline{7A}})}{s_{789}} + \frac{(s_{89} + s_{9A})(s_{67} + s_{\overline{7A}})}{s_{89A}} \right] \\
&+ s_{\overline{47}} + s_{\overline{58}} + s_{\overline{69}} + s_{\overline{7A}} + \left. \frac{(s_{\overline{7A}} + s_{\overline{A3}})(s_{45} + s_{56})(s_{78} + s_{89})}{s_{456} s_{789}} \right\} + [\mathbb{Z}_{10}]. \tag{E.10}
\end{aligned}$$

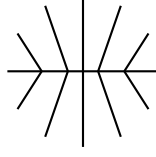
To avoid problems with multi-digit indices, we switch to hexadecimal and write A instead of 10. To abbreviate long index lists, we write  $\overline{ij}$  for  $i(i+1)\cdots(j-1)j$ . Indices wrap around cyclically;  $\overline{A3}$  means A123.

### E.3 The $\mathcal{O}(p^2)$ 12-point amplitude

This is a novel amplitude, and takes the most time to compute of all amplitudes presented in this work. It consists of 73 diagrams:







and has the stripped amplitude

$$\begin{aligned}
& -32iF^{10}\mathcal{M}_{2,\{12\}} = 14s_{12} + 5s_{1234} + 2s_{123456} \\
& + \frac{s_{12} + \dots + s_{45} + s_{\overline{14}} + s_{\overline{25}}}{s_{\overline{15}}} \left\{ - \frac{(s_{67} + \dots + s_{9A} + s_{\overline{69}} + s_{\overline{7A}})(s_{\overline{69}} + s_{\overline{7A}})}{s_{\overline{6A}}} \right. \\
& \quad \times [2(s_{67} + \dots + s_{BC}) + (s_{\overline{69}} + \dots + s_{\overline{9C}}) + 2(s_{\overline{16}} + s_{\overline{6B}})] \\
& \quad \left. + \frac{(s_{78} + \dots + s_{AB} + s_{\overline{7A}} + s_{\overline{8B}})(s_{\overline{16}} + s_{\overline{6B}})}{2s_{\overline{7B}}} \right\} \\
& + \frac{s_{12} + s_{23}}{s_{123}} \left\{ - [5(s_{45} + \dots + s_{BC} + s_{\overline{C3}} + s_{\overline{14}}) + 2(s_{47} + \dots + s_{\overline{9C}} + s_{49} + \dots + s_{7C})] \right. \\
& + \frac{s_{45} + s_{56}}{s_{456}} \left[ 2(s_{78} + \dots + s_{BC} + s_{\overline{C3}} + s_{47} + s_{\overline{16}}) + s_{\overline{7A}} + s_{\overline{8B}} + s_{\overline{9C}} + s_{49} \right. \\
& \quad + \frac{s_{78} + s_{89}}{s_{789}} \left( - [s_{AB} + s_{BC} + s_{\overline{7A}} + s_{\overline{C3}} + s_{\overline{16}} + s_{49}] + \frac{s_{AB} + s_{BC}}{2s_{ABC}} \right. \\
& \quad \left. \left. + \frac{(s_{\overline{7A}} + s_{AB})(s_{\overline{16}} + s_{\overline{C3}})}{s_{\overline{7B}}} + \frac{(s_{\overline{7A}} + s_{49})(s_{BC} + s_{\overline{C3}})}{s_{\overline{B3}}} \right) \right. \\
& \quad + \frac{s_{89} + s_{9A}}{s_{89A}} \left( - [s_{BC} + s_{47} + s_{\overline{7A}} + s_{\overline{8B}} + s_{\overline{C3}} + s_{\overline{16}}] + \frac{(s_{\overline{7A}} + s_{\overline{8B}})(s_{\overline{C3}} + s_{\overline{16}})}{s_{\overline{7B}}} \right. \\
& \quad \left. \left. + \frac{(s_{\overline{8B}} + s_{\overline{BC}})(s_{47} + s_{\overline{16}})}{s_{\overline{8C}}} + \frac{(s_{\overline{BC}} + s_{\overline{C3}})(s_{47} + s_{\overline{7A}})}{s_{\overline{B3}}} \right) \right. \\
& \quad + \frac{s_{9A} + s_{AB}}{s_{9AB}} \left( - [s_{47} + s_{78} + s_{\overline{9C}} + s_{\overline{C3}} + s_{\overline{16}}] + \frac{(s_{47} + s_{78})(s_{\overline{9C}} + s_{\overline{C3}})}{s_{48}} \right. \\
& \quad \left. \left. + \frac{(s_{78} + s_{\overline{8B}})(s_{\overline{C3}} + s_{\overline{16}})}{s_{\overline{7B}}} + \frac{(s_{\overline{8B}} + s_{\overline{9C}})(s_{47} + s_{\overline{16}})}{s_{\overline{8C}}} \right) \right. \\
& \quad + \frac{s_{47} + s_{78}}{s_{48}} \left( \frac{(s_{49} + s_{9A})(s_{BC} + s_{\overline{C3}})}{s_{\overline{B3}}} - [s_{9A} + s_{AB} + s_{BC} + s_{\overline{9C}} + s_{\overline{C3}} + s_{49}] \right) \\
& \quad - \frac{(s_{\overline{C3}} + s_{\overline{16}})(s_{78} + \dots + s_{AB} + s_{\overline{7A}} + s_{\overline{8B}})}{s_{\overline{7B}}} \\
& \quad - \frac{(s_{47} + s_{\overline{16}})(s_{89} + \dots + s_{BC} + s_{8B} + s_{\overline{9C}})}{s_{8C}} \\
& \quad \left. - \frac{(s_{BC} + s_{\overline{C3}})(s_{78} + s_{89} + s_{9A} + s_{47} + s_{\overline{7A}} + s_{49})}{s_{\overline{B3}}} \right] \\
& + \frac{s_{56} + s_{67}}{s_{567}} \left[ 2(s_{89} + \dots + s_{BC} + s_{\overline{C3}} + s_{\overline{14}} + s_{47} + s_{58}) + s_{\overline{8B}} + s_{\overline{9C}} + s_{49} + s_{5A} \right. \\
& \quad \left. + \frac{s_{9A} + s_{AB}}{s_{9AB}} \left( \frac{(s_{47} + s_{58})(s_{\overline{9C}} + s_{\overline{C3}})}{s_{48}} - 1 \right) \right]
\end{aligned}$$

$$\begin{aligned}
& + \frac{s_{47} + s_{58}}{s_{48}} \left( \frac{(s_{49} + s_{9A})(s_{BC} + s_{C3})}{s_{B3}} - (s_{9A} + s_{AB} + s_{BC} + s_{9C} + s_{C3} + s_{49}) \right) \\
& + \frac{s_{58} + s_{89}}{s_{59}} \left( \frac{(s_{BC} + s_{C3})(s_{49} + s_{5A})}{s_{B3}} + \frac{(s_{C3} + s_{14})(s_{5A} + s_{AB})}{s_{C4}} \right. \\
& \quad \left. - (s_{AB} + s_{BC} + s_{C3} + s_{14} + s_{49} + s_{5A}) \right) \\
& - \frac{(s_{14} + s_{47})(s_{89} + \dots + s_{BC} + s_{8B} + s_{9C})}{s_{8C}} \\
& - \frac{(s_{BC} + s_{C3})(s_{89} + s_{9A} + s_{47} + s_{58} + s_{49} + s_{5A})}{s_{B3}} \\
& - \left. \frac{(s_{C3} + s_{14})(s_{89} + s_{9A} + s_{AB} + s_{58} + s_{8B} + s_{5A})}{s_{C4}} \right] \\
& + \frac{s_{67} + s_{78}}{s_{678}} \left[ 2(s_{45} + s_{9A} + s_{AB} + s_{BC} + s_{C3} + s_{14} + s_{58} + s_{69}) + s_{9C} + s_{49} + s_{5A} + s_{6B} \right. \\
& \quad + \frac{s_{45} + s_{14}}{s_{15}} \left( \frac{(s_{69} + s_{9A})(s_{6B} + s_{BC})}{s_{6A}} - (s_{9A} + s_{AB} + s_{BC} + s_{69} + s_{9C} + s_{6B}) \right) \\
& \quad + \frac{s_{45} + s_{58}}{s_{48}} \left( \frac{(s_{49} + s_{9A})(s_{BC} + s_{C3})}{s_{B3}} - (s_{9A} + s_{AB} + s_{BC} + s_{9C} + s_{C3} + s_{49}) \right) \\
& \quad + \frac{s_{58} + s_{69}}{s_{59}} \left( \frac{(s_{BC} + s_{C3})(s_{49} + s_{5A})}{s_{B3}} + \frac{(s_{C3} + s_{14})(s_{5A} + s_{AB})}{s_{C4}} \right. \\
& \quad \left. - (s_{AB} + s_{BC} + s_{C3} + s_{14} + s_{49} + s_{5A}) \right) \\
& \quad + \frac{s_{69} + s_{9A}}{s_{6A}} \left( \frac{(s_{45} + s_{5A})(s_{BC} + s_{C3})}{s_{B3}} + \frac{(s_{C3} + s_{14})(s_{5A} + s_{6B})}{s_{C4}} \right. \\
& \quad \left. - (s_{BC} + s_{C3} + s_{14} + s_{5A} + s_{6B}) \right) \\
& \quad - \frac{(s_{BC} + s_{C3})(s_{45} + s_{BC} + s_{58} + s_{69} + s_{49} + s_{5A})}{s_{B3}} \\
& \quad \left. - \frac{(s_{C3} + s_{14})(s_{9A} + s_{AB} + s_{58} + s_{69} + s_{5A} + s_{6B})}{s_{C4}} \right] \\
& + \frac{s_{78} + s_{89}}{s_{789}} \left[ \frac{1}{2}(s_{45} + s_{56} + s_{14} + s_{69}) + 2(s_{16} + s_{49} + s_{5A} + s_{6B}) \right. \\
& \quad + \frac{s_{14} + s_{45}}{s_{15}} \left( \frac{(s_{6B} + s_{BC})(s_{69} + s_{7A})}{s_{6A}} + \frac{(s_{7A} + s_{AB})(s_{16} + s_{6B})}{2s_{7B}} \right. \\
& \quad \left. - (s_{AB} + s_{BC} + s_{69} + s_{7A} + s_{16} + s_{6B}) \right) \\
& \quad + \frac{s_{56} + s_{69}}{s_{59}} \left( \frac{(s_{BC} + s_{C3})(s_{49} + s_{5A})}{2s_{B3}} + \frac{(s_{C3} + s_{14})(s_{5A} + s_{AB})}{s_{C4}} \right. \\
& \quad \left. - (s_{AB} + s_{BC} + s_{C3} + s_{14} + s_{49} + s_{5A}) \right) \\
& \quad \left. + \frac{s_{69} + s_{7A}}{s_{6A}} \left( \frac{(s_{C3} + s_{14})(s_{5A} + s_{6B})}{2s_{C4}} - (s_{45} + s_{BC} + s_{C3} + s_{14} + s_{5A} + s_{6B}) \right) \right]
\end{aligned}$$

$$\begin{aligned}
& + \frac{s_{\overline{14}} + s_{45}}{s_{\overline{15}}} \left[ 2 (s_{67} + \dots + s_{BC} + s_{\overline{16}} + s_{\overline{6B}}) + s_{\overline{69}} + \dots + s_{\overline{9C}} \right. \\
& \quad - \frac{(s_{\overline{6B}} + s_{BC})(s_{67} + \dots + s_{9A} + s_{\overline{69}} + s_{\overline{7A}})}{s_{\overline{6A}}} \\
& \quad - \frac{(s_{\overline{16}} + s_{\overline{6B}})(s_{78} + \dots + s_{AB} + s_{\overline{7A}} + s_{\overline{8B}})}{s_{\overline{7B}}} \\
& \quad \left. - \frac{(s_{\overline{16}} + s_{67})(s_{89} + \dots + s_{BC} + s_{\overline{8B}} + s_{\overline{9C}})}{s_{\overline{8C}}} \right] \\
& + \frac{s_{45} + \dots + s_{78} + s_{\overline{47}} + s_{\overline{58}}}{s_{\overline{48}}} \left[ (s_{9A} + s_{AB} + s_{BC} + s_{\overline{9C}} + s_{\overline{C3}} + s_{\overline{49}}) \right. \\
& \quad \left. - \frac{(s_{\overline{49}} + s_{9A})(s_{BC} + s_{\overline{C3}})}{s_{\overline{B3}}} \right] \\
& + \frac{s_{56} + \dots + s_{89} + s_{\overline{58}} + s_{\overline{69}}}{s_{\overline{59}}} \left[ (s_{AB} + s_{BC} + s_{\overline{C3}} + s_{\overline{14}} + s_{\overline{49}} + s_{\overline{5A}}) \right. \\
& \quad \left. - \frac{(s_{\overline{49}} + s_{\overline{5A}})(s_{BC} + s_{\overline{C3}})}{s_{\overline{B3}}} - \frac{(s_{\overline{5A}} + s_{\overline{AB}})(s_{\overline{C3}} + s_{\overline{14}})}{s_{\overline{C4}}} \right] \\
& + \frac{s_{67} + \dots + s_{9A} + s_{\overline{69}} + s_{\overline{7A}}}{s_{\overline{6A}}} \left[ (s_{45} + s_{BC} + s_{\overline{C3}} + s_{\overline{14}} + s_{\overline{5A}} + s_{\overline{6B}}) \right. \\
& \quad \left. - \frac{(s_{\overline{45}} + s_{\overline{5A}})(s_{BC} + s_{\overline{C3}})}{s_{\overline{B3}}} - \frac{(s_{\overline{C3}} + s_{\overline{14}})(s_{\overline{5A}} + s_{\overline{6B}})}{s_{\overline{C4}}} \right] \\
& + \frac{s_{78} + \dots + s_{AB} + s_{\overline{7A}} + s_{\overline{8B}}}{s_{\overline{7B}}} \left[ (s_{45} + s_{56} + s_{\overline{C3}} + s_{\overline{14}} + s_{\overline{16}} + s_{\overline{6B}}) - \frac{(s_{\overline{C3}} + s_{\overline{14}})(s_{56} + s_{\overline{6B}})}{s_{\overline{C4}}} \right] \\
& + \frac{(s_{89} + \dots + s_{BC} + s_{\overline{8B}} + s_{\overline{9C}})(s_{56} + s_{67} + s_{\overline{14}} + s_{\overline{47}} + s_{\overline{16}})}{s_{\overline{8C}}} \\
& + \frac{(s_{BC} + s_{\overline{C3}}) [2(s_{45} + \dots + s_{9A} + s_{\overline{49}} + s_{\overline{9A}}) + s_{\overline{47}} + \dots + s_{\overline{7A}}]}{s_{\overline{B3}}} \\
& + \left. \frac{(s_{\overline{C3}} + s_{\overline{14}}) [2(s_{56} + \dots + s_{AB} + s_{\overline{5A}} + s_{\overline{6B}}) + s_{\overline{58}} + \dots + s_{\overline{8B}}]}{s_{\overline{C4}}} \right\} + [\mathbb{Z}_{12}]. \quad (\text{E.11})
\end{aligned}$$

We use the same abbreviations as above, with A, B, C = 10, 11, 12. Furthermore, we contract sums like  $s_{12} + s_{23} + s_{34} + s_{45}$  to  $s_{12} + \dots + s_{45}$ .

## References

- [1] M. Gell-Mann and M. Levy, *The axial vector current in beta decay*, *Nuovo Cim.* **16** (1960) 705.
- [2] S. Weinberg, *Phenomenological Lagrangians*, *Physica* **A96** (1979) 327.
- [3] J. Gasser and H. Leutwyler, *Chiral Perturbation Theory to One Loop*, *Annals Phys.* **158** (1984) 142.
- [4] J. Gasser and H. Leutwyler, *Chiral Perturbation Theory: Expansions in the Mass of the Strange Quark*, *Nucl. Phys.* **B250** (1985) 465.

- [5] A. Pich, *Effective Field Theory with Nambu-Goldstone Modes*, in *Les Houches summer school: EFT in Particle Physics and Cosmology Les Houches, Chamonix Valley, France, July 3-28, 2017*, 2018, [1804.05664](#).
- [6] <http://home.thep.lu.se/~bijnens/chpt/>.
- [7] J. Bijnens and J. Lu, *Meson-meson Scattering in QCD-like Theories*, *JHEP* **03** (2011) 028 [[1102.0172](#)].
- [8] J. Bijnens and N. Hermansson Truedsson, *The Pion Mass and Decay Constant at Three Loops in Two-Flavour Chiral Perturbation Theory*, *JHEP* **11** (2017) 181 [[1710.01901](#)].
- [9] H. Elvang and Y.-t. Huang, *Scattering Amplitudes*, [1308.1697](#).
- [10] K. Kampf, J. Novotny and J. Trnka, *Recursion relations for tree-level amplitudes in the  $SU(N)$  nonlinear sigma model*, *Phys. Rev.* **D87** (2013) 081701 [[1212.5224](#)].
- [11] C. Cheung, K. Kampf, J. Novotny, C.-H. Shen and J. Trnka, *On-Shell Recursion Relations for Effective Field Theories*, *Phys. Rev. Lett.* **116** (2016) 041601 [[1509.03309](#)].
- [12] S. L. Adler, *Consistency conditions on the strong interactions implied by a partially conserved axial vector current*, *Phys. Rev.* **137** (1965) B1022.
- [13] C. Cheung, K. Kampf, J. Novotny, C.-H. Shen and J. Trnka, *A Periodic Table of Effective Field Theories*, *JHEP* **02** (2017) 020 [[1611.03137](#)].
- [14] H. Elvang, M. Hadjiantonis, C. R. T. Jones and S. Paranjape, *Soft Bootstrap and Supersymmetry*, *JHEP* **01** (2019) 195 [[1806.06079](#)].
- [15] I. Low and Z. Yin, *Soft Bootstrap and Effective Field Theories*, [1904.12859](#).
- [16] H. Osborn, *Implications of adler zeros for multipion processes*, *Lett. Nuovo Cim.* **2S1** (1969) 717.
- [17] L. Susskind and G. Frye, *Algebraic aspects of pionic duality diagrams*, *Phys. Rev.* **D1** (1970) 1682.
- [18] J. R. Ellis and B. Renner, *On the relationship between chiral and dual models*, *Nucl. Phys.* **B21** (1970) 205.
- [19] F. Cachazo, S. He and E. Y. Yuan, *Scattering Equations and Matrices: From Einstein To Yang-Mills, DBI and NLSM*, *JHEP* **07** (2015) 149 [[1412.3479](#)].
- [20] H. Gomez and A. Helset, *Scattering equations and a new factorization for amplitudes. Part II. Effective field theories*, *JHEP* **05** (2019) 129 [[1902.02633](#)].
- [21] G. Chen and Y.-J. Du, *Amplitude Relations in Non-linear Sigma Model*, *JHEP* **01** (2014) 061 [[1311.1133](#)].
- [22] G. Chen, Y.-J. Du, S. Li and H. Liu, *Note on off-shell relations in nonlinear sigma model*, *JHEP* **03** (2015) 156 [[1412.3722](#)].
- [23] Y.-J. Du and H. Luo, *On single and double soft behaviors in NLSM*, *JHEP* **08** (2015) 058 [[1505.04411](#)].
- [24] I. Low, *Double Soft Theorems and Shift Symmetry in Nonlinear Sigma Models*, *Phys. Rev.* **D93** (2016) 045032 [[1512.01232](#)].
- [25] Y.-J. Du and C.-H. Fu, *Explicit BCJ numerators of nonlinear sigma model*, *JHEP* **09** (2016) 174 [[1606.05846](#)].

- [26] J. J. M. Carrasco, C. R. Mafra and O. Schlotterer, *Abelian Z-theory: NLSM amplitudes and  $\alpha'$ -corrections from the open string*, *JHEP* **06** (2017) 093 [[1608.02569](#)].
- [27] Y.-J. Du and H. Luo, *Leading order multi-soft behaviors of tree amplitudes in NLSM*, *JHEP* **03** (2017) 062 [[1611.07479](#)].
- [28] C. Cheung, G. N. Remmen, C.-H. Shen and C. Wen, *Pions as Gluons in Higher Dimensions*, *JHEP* **04** (2018) 129 [[1709.04932](#)].
- [29] I. Low and Z. Yin, *Ward Identity and Scattering Amplitudes for Nonlinear Sigma Models*, *Phys. Rev. Lett.* **120** (2018) 061601 [[1709.08639](#)].
- [30] I. Low and Z. Yin, *The Infrared Structure of Nambu-Goldstone Bosons*, *JHEP* **10** (2018) 078 [[1804.08629](#)].
- [31] L. Rodina, *Scattering Amplitudes from Soft Theorems and Infrared Behavior*, *Phys. Rev. Lett.* **122** (2019) 071601 [[1807.09738](#)].
- [32] S. Mizera and B. Skrzypek, *Perturbative Methods for Effective Field Theories and the Double Copy*, *JHEP* **10** (2018) 018 [[1809.02096](#)].
- [33] N. E. J. Bjerrum-Bohr, H. Gomez and A. Helset, *New factorization relations for nonlinear sigma model amplitudes*, *Phys. Rev.* **D99** (2019) 045009 [[1811.06024](#)].
- [34] D. T. Cornwell, *The six pion amplitude to fourth order in momenta*, *Nucl. Phys.* **B34** (1971) 125.
- [35] M. Carrillo-Gonzalez, R. Penco and M. Trodden, *Shift symmetries, soft limits, and the double copy beyond leading order*, [1908.07531](#).
- [36] K. Kampf, J. Novotny and J. Trnka, *Tree-level Amplitudes in the Nonlinear Sigma Model*, *JHEP* **05** (2013) 032 [[1304.3048](#)].
- [37] M. Sjö, *Flavour-ordering in the nonlinear sigma model with more derivatives and legs*, Master thesis LU TP 19-21, Lund University, June 2019.
- [38] File `flavour-order.pdf` included with this submission.
- [39] G. Ecker, J. Gasser, A. Pich and E. de Rafael, *The Role of Resonances in Chiral Perturbation Theory*, *Nucl. Phys.* **B321** (1989) 311.
- [40] J. Bijnens, G. Colangelo and G. Ecker, *The Mesonic chiral Lagrangian of order  $p^6$* , *JHEP* **02** (1999) 020 [[hep-ph/9902437](#)].
- [41] J. Bijnens, N. Hermansson-Truedsson and S. Wang, *The order  $p^8$  mesonic chiral Lagrangian*, *JHEP* **01** (2019) 102 [[1810.06834](#)].
- [42] C. Reuschle and S. Weinzierl, *Decomposition of one-loop QCD amplitudes into primitive amplitudes based on shuffle relations*, *Phys. Rev.* **D88** (2013) 105020 [[1310.0413](#)].
- [43] T. Schuster, *Color ordering in QCD*, *Phys. Rev.* **D89** (2014) 105022 [[1311.6296](#)].
- [44] M. L. Mangano and S. J. Parke, *Multiparton amplitudes in gauge theories*, *Phys. Rept.* **200** (1991) 301 [[hep-th/0509223](#)].
- [45] M. Sjö Dahl and J. Thorén, *Decomposing color structure into multiplet bases*, *JHEP* **09** (2015) 055 [[1507.03814](#)].
- [46] S. Weinberg, *The quantum theory of fields*, vol. 2. Cambridge university press, 1996.

- [47] C. Cheung, K. Kampf, J. Novotný and J. Trnka, *Effective Field Theories from Soft Limits of Scattering Amplitudes*, *Phys. Rev. Lett.* **114** (2015) 221602 [[1412.4095](#)].
- [48] N. Arkani-Hamed, F. Cachazo and J. Kaplan, *What is the Simplest Quantum Field Theory?*, *JHEP* **09** (2010) 016 [[0808.1446](#)].
- [49] J. A. M. Vermaseren, *New features of FORM*, [math-ph/0010025](#).
- [50] J. Kuipers, T. Ueda, J. A. M. Vermaseren and J. Vollinga, *FORM version 4.0*, *Comput. Phys. Commun.* **184** (2013) 1453 [[1203.6543](#)].
- [51] J. Bijnens and L. Carloni, *The Massive  $O(N)$  Non-linear Sigma Model at High Orders*, *Nucl. Phys.* **B843** (2011) 55 [[1008.3499](#)].
- [52] J. Bijnens, K. Kampf and S. Lanz, *Leading logarithms in  $N$ -flavour mesonic Chiral Perturbation Theory*, *Nucl. Phys.* **B873** (2013) 137 [[1303.3125](#)].
- [53] J. Bijnens, G. Colangelo and G. Ecker, *Renormalization of chiral perturbation theory to order  $p^6$* , *Annals Phys.* **280** (2000) 100 [[hep-ph/9907333](#)].